Particle production and hypernucleus formation in heavy-ion collisions

Zhao-Qing Feng (冯兆庆)

South China University of Technology, Guangzhou

Outline

- Introduction
- Particle production in heavy-ion collisions and in hadron induced reactions near threshold energies
- In-medium and isospin effects on particle production (π, η, K, Λ, Σ, Ξ)
- Hypernuclear formation
- Summary

I. Introduction

H. Tamura, *Prog. Theor. Exp. Phys.* (2012) 02B012

Advantages of heavy-ion collisions on hypernucleus production

1. Neutron-rich/proton-rich hypernuclear isotopes
2. Hypernucleus with s=-2 by capturing $\Xi^{-,0}$ by nucleonic fragments
3. Λ-Λ correlation in dense nuclear matter

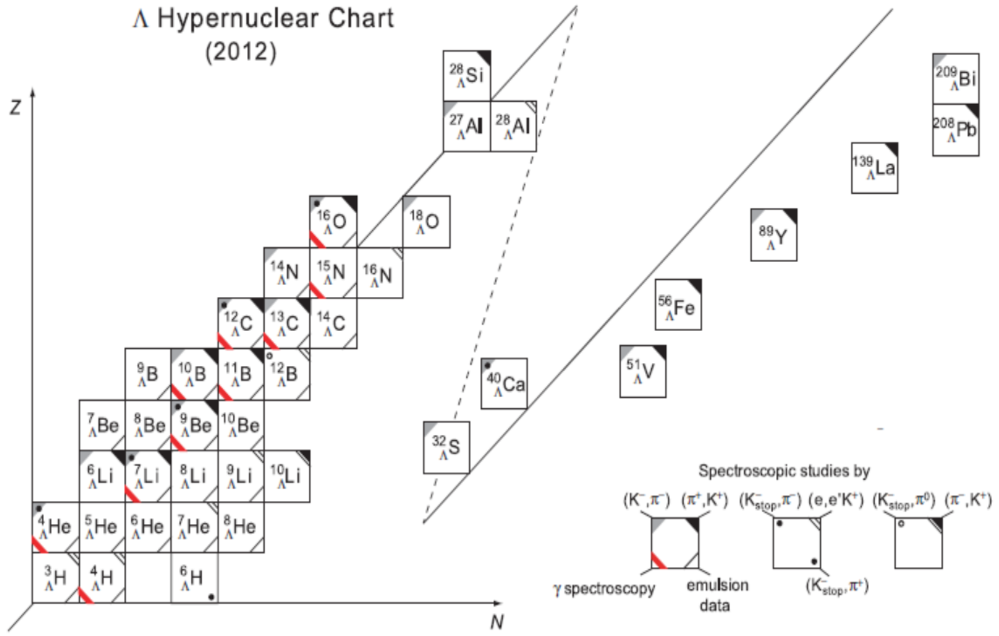

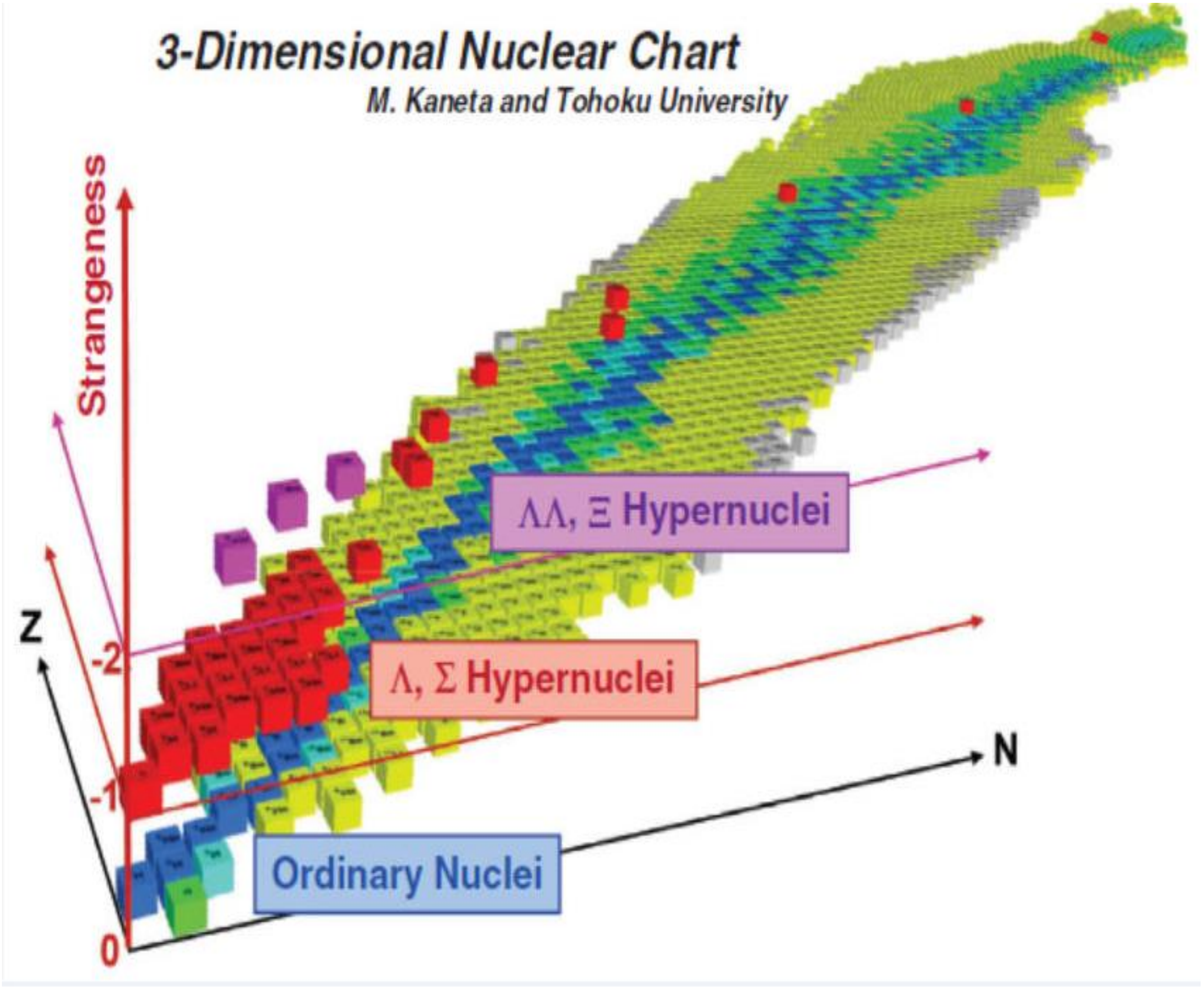

A. Andronic, P. Braun-Munzinger, J. Stachel, H. Stöcker, Physics Letters B 697 (2011) 203–207

A.S.Botvina, J.Steinheimer, E.Bratkovskaya, M.Bleicher, J.Pochodzalla, Physics Letters B 742 (2015)7–14

Pb+Pb

statistical model

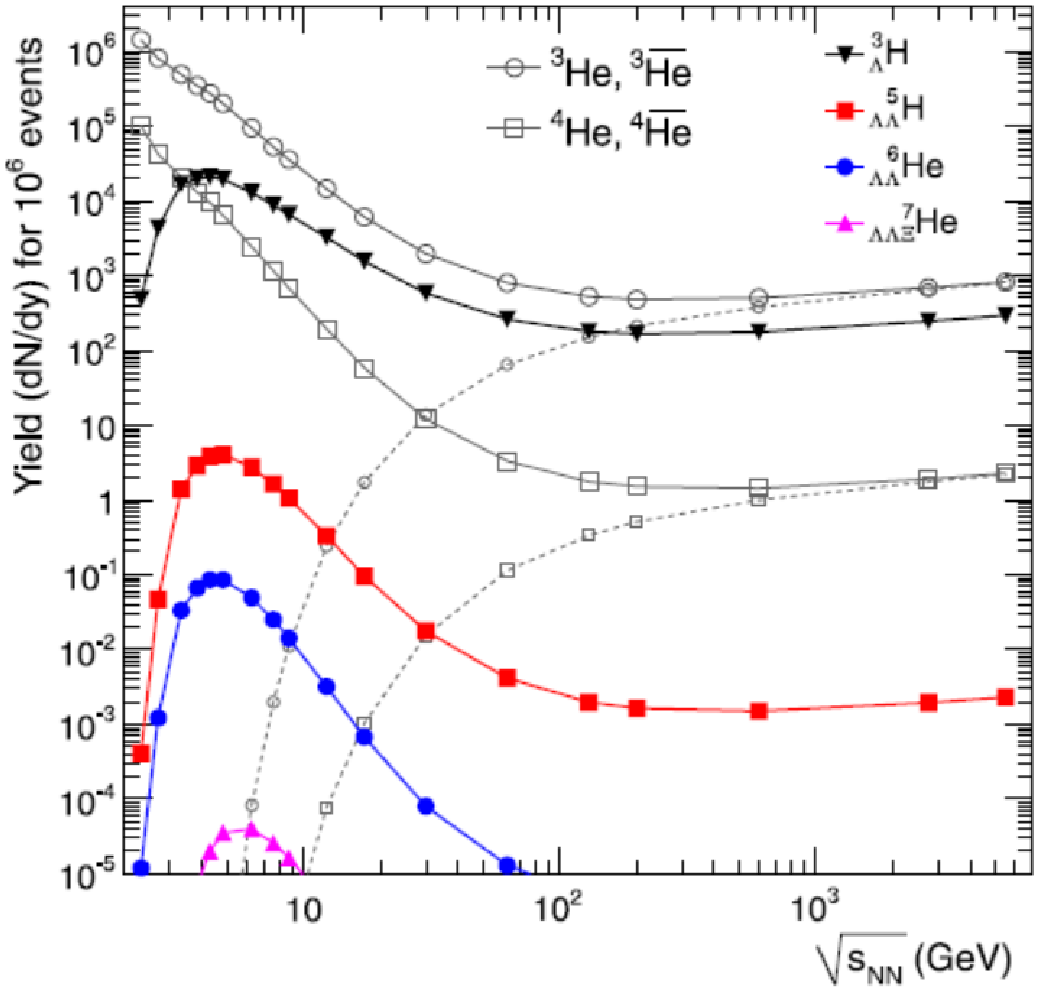

transport model+coalescence approach

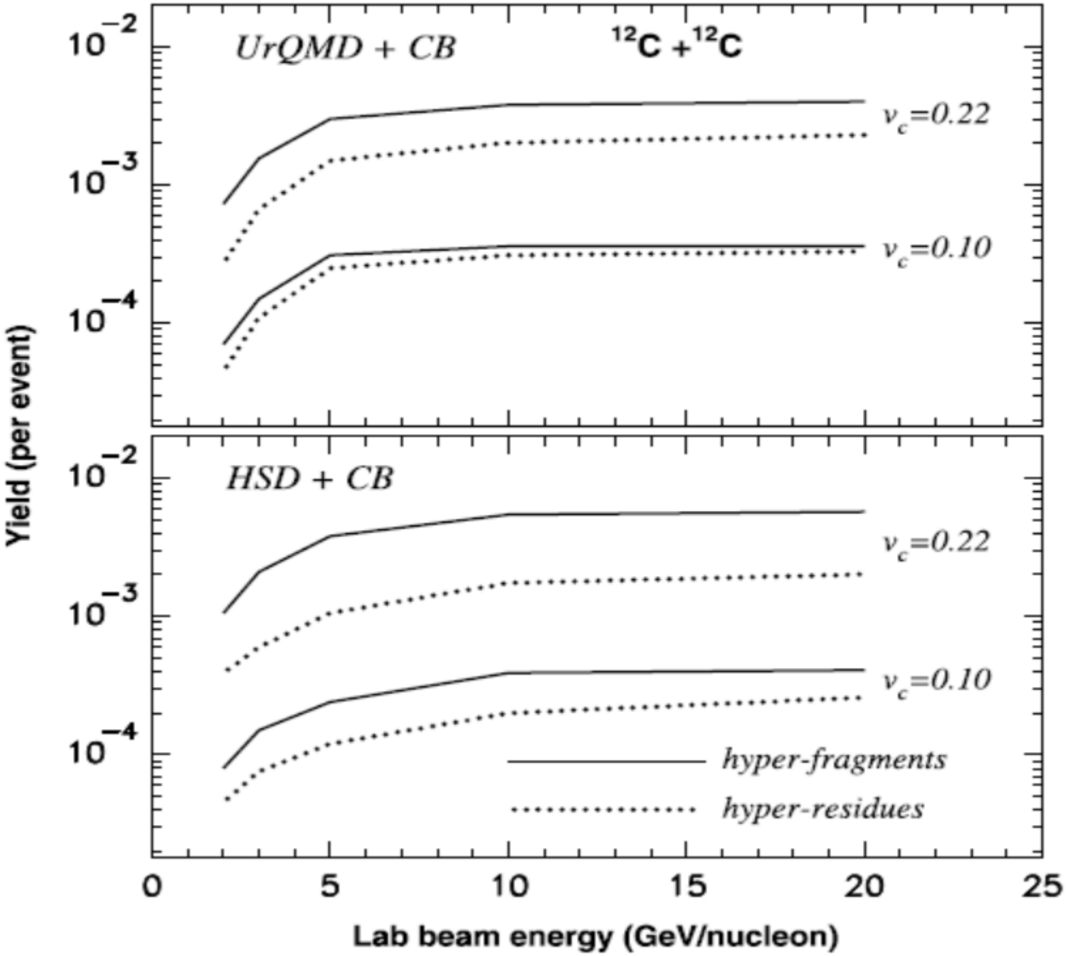

home.cern/about/accelerators/low-energy-antiproton-ring

Low Energy Antiproton Ring at CERN (1982-1996)

Proton Synchrotron (PS), Antiproton Collector (AC), Antiproton Accumulator (AA)

Physics: highly excited nucleus, delayed fission process, cold QGP, hadrons in-medium …

PANDA detector from http://www-panda.gsi.de/

PANDA(antiProton ANnihilation at Darmstadt)

Physics purpose:

Hadron Spectroscopy, Nucleon Structure,

Hadron in Baryonic Matter, Hypernucleus

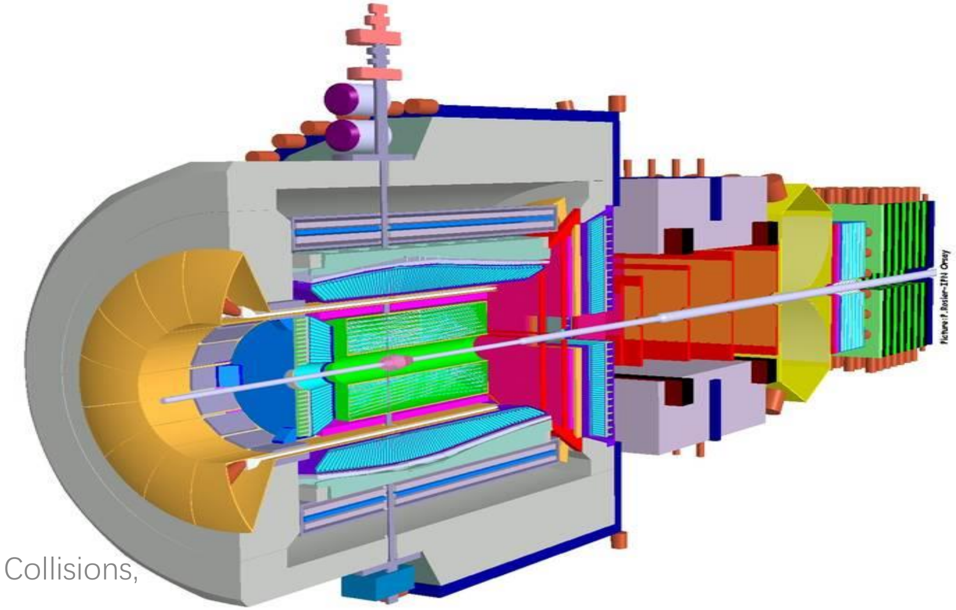

HIAF (High-Intensity Heavy Ion Accelerator Facility)

Provided by Jian-Cheng Yang

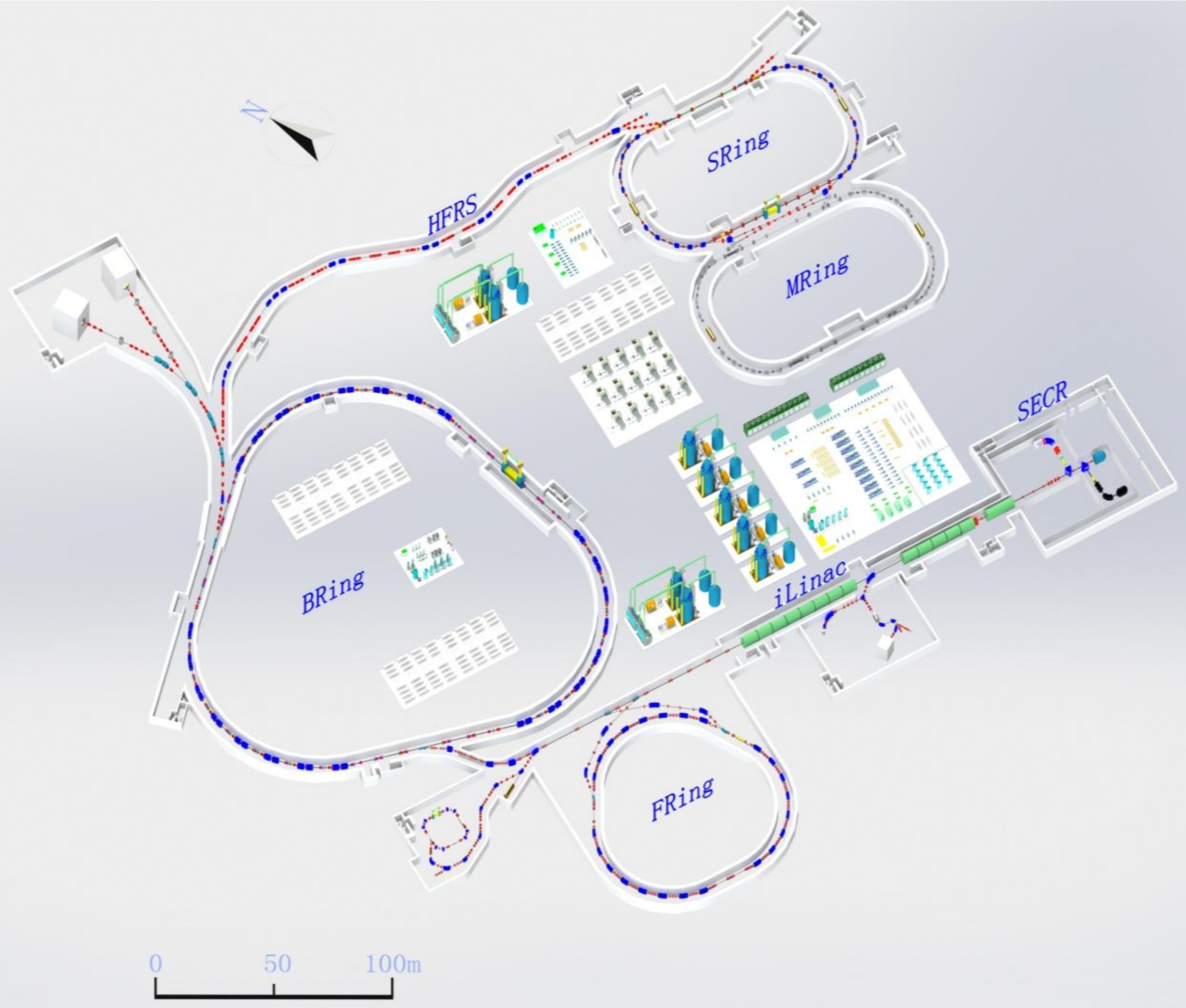

	Ions	Energy	Intensity
SECR	$^{238}U^{35+}$	14 keV/u	0.05-0.1 pmA
iLinac	$^{238}U^{35+}$	17 MeV/u	0.028-0.05 pmA
FRing	$^{238}U^{35+}$	0.35 GeV/u	~2.0×10^{11} ppp
BRing	$^{238}U^{35+}$	1.0 GeV/u	~1.0×10^{12} ppp
	$^{238}U^{92+}$	**3.8 GeV/u**	**~5.0×10^{11} ppp**
SRing	RIBs: **neutron-rich, proton-rich**	0.84 GeV/u(A/q=3)	~10^{9-10} ppp
	Fully stripped heavy ions H-like, He-like heavy ions	0.8 GeV/u($^{238}U^{92+}$)	~10^{11-12} ppp

II. Model description

Lanzhou Quantum Molecular Dynamics (LQMD) transport model

Nuclear dynamics from 15 MeV/nucleon – 5 GeV/nucleon for HICs, antiproton (proton, π, K, etc)

- **Dynamics of low-energy heavy-ion collisions** (dynamical interaction potential, barrier distribution, neck dynamics, fusion/caption excitation functions etc)
- **Isospin physics at intermediate energies** (constraining nuclear symmetry energy at sub- and supra-saturation densities in HICs and probing isospin splitting of nucleon effective mass from HICs)
- **In-medium properties of hadrons in dense nuclear matter from heavy-ion collisions** (extracting optical potentials, i.e., Δ(1232), N*(1440), N*(1535)), hyperons (Λ,Σ,Ξ,Ω) and mesons (π,K,η,ρ,ω,ϕ…), hypernucleus dynamics)
- **Hadron (antiproton, proton, $\pi^{\pm}$, $K^{\pm}$) induced reactions** (hypernucleus production, e.g., Λ(Σ)X, ΛΛX, ΞX, $\bar{\Lambda}$X(S=1), in-medium modifications of hadrons, cold QGP)

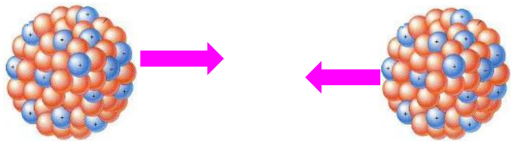

Density, isospin and momentum-dependent single-nucleon potential in LQMD

$$U_\tau(\rho,\delta,\mathbf{p}) = \alpha\frac{\rho}{\rho_0} + \beta\frac{\rho^\gamma}{\rho_0^\gamma} + E_{\rm sym}^{\rm loc}(\rho)\delta^2 + \frac{\partial E_{\rm sym}^{\rm loc}(\rho)}{\partial\rho}\rho\delta^2 + E_{\rm sym}^{\rm loc}(\rho)\rho\frac{\partial\delta^2}{\partial\rho_\tau}$$
$$+ \frac{1}{\rho_0}C_{\tau,\tau}\int d\mathbf{p}' f_\tau(\mathbf{r},\mathbf{p})[\ln(\epsilon(\mathbf{p}-\mathbf{p}')^2+1)]^2$$
$$+ \frac{1}{\rho_0}C_{\tau,\tau'}\int d\mathbf{p}' f_{\tau'}(\mathbf{r},\mathbf{p})[\ln(\epsilon(\mathbf{p}-\mathbf{p}')^2+1)]^2.$$

$$C_{\tau,\tau} = C_{mom}(1+x),\ C_{\tau,\tau'} = C_{mom}(1-x)\ \ (\tau\neq\tau')$$

ZQF, Phys. Rev. C 84 (2011) 024610

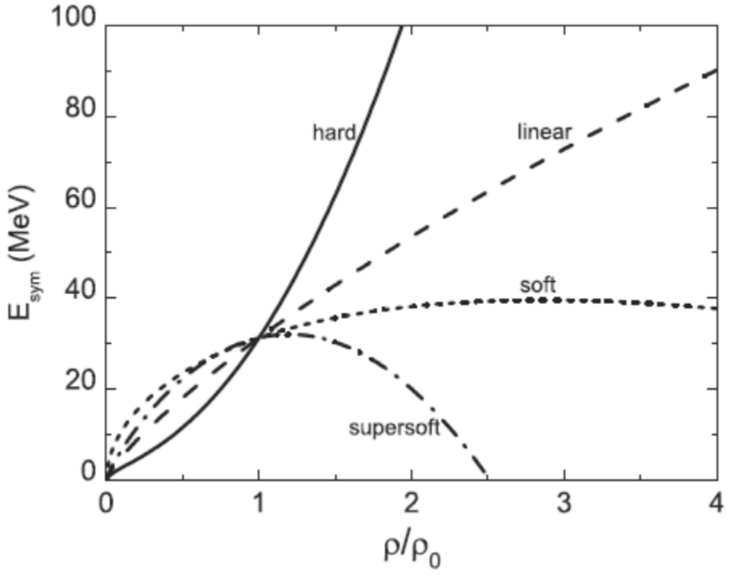

Table 1: The parameters and properties of isospin symmetric EoS used in the LQMD model at the density of 0.16 fm^{-3}.

Parameters	α (MeV)	β (MeV)	γ	C_{mom} (MeV)	ϵ (c^2/MeV^2)	m^*_∞/m	K_∞ (MeV)
PAR1	-215.7	142.4	1.322	1.76	5×10^{-4}	0.75	230
PAR2	-226.5	173.7	1.309	0.	0.	1.	230

Isospin splitting of nucleon effective mass on isospin emissions in heavy-ion collisions

(Nucl. Phys. A 878 (2012) 3)

$$\frac{m_\tau^*}{m} = \left[1 + \frac{m}{\hbar^2 k}\frac{\partial U_\tau}{\partial k}\right]^{-1}$$

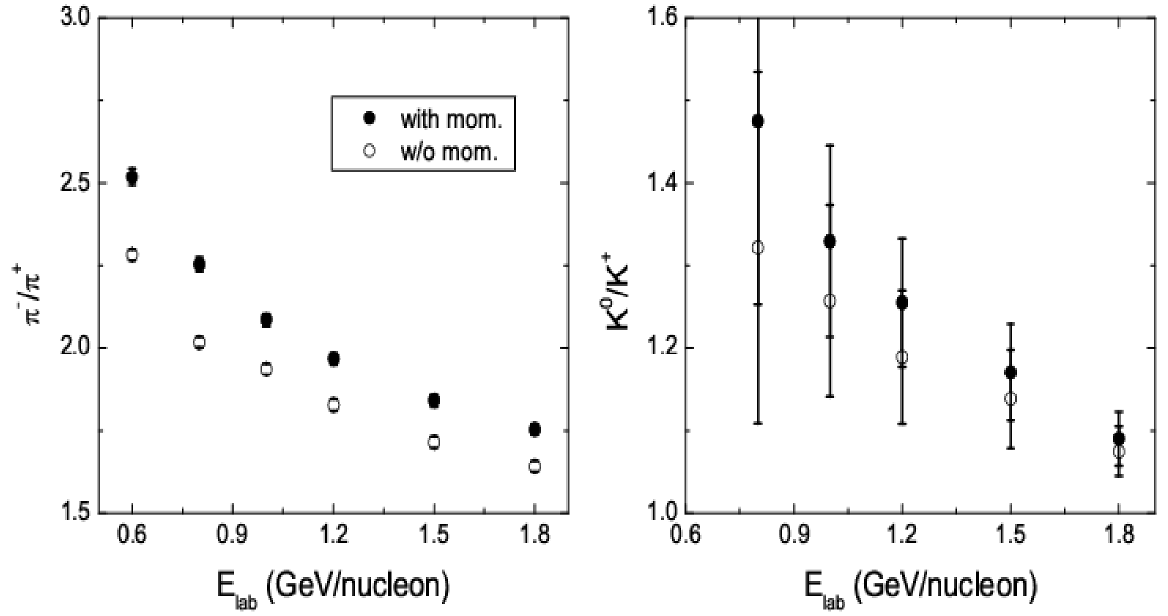

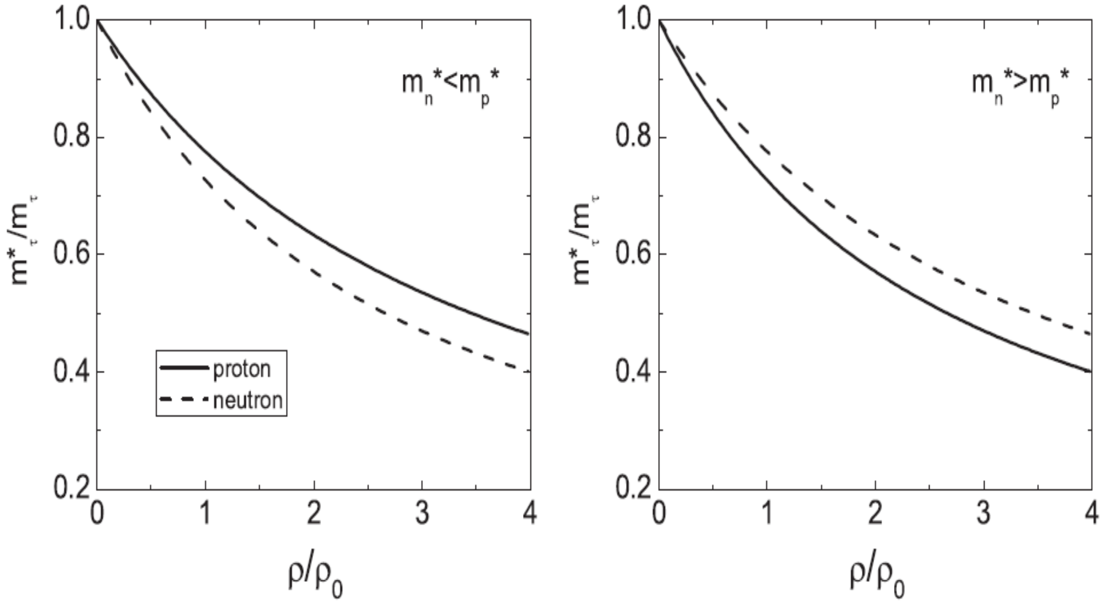

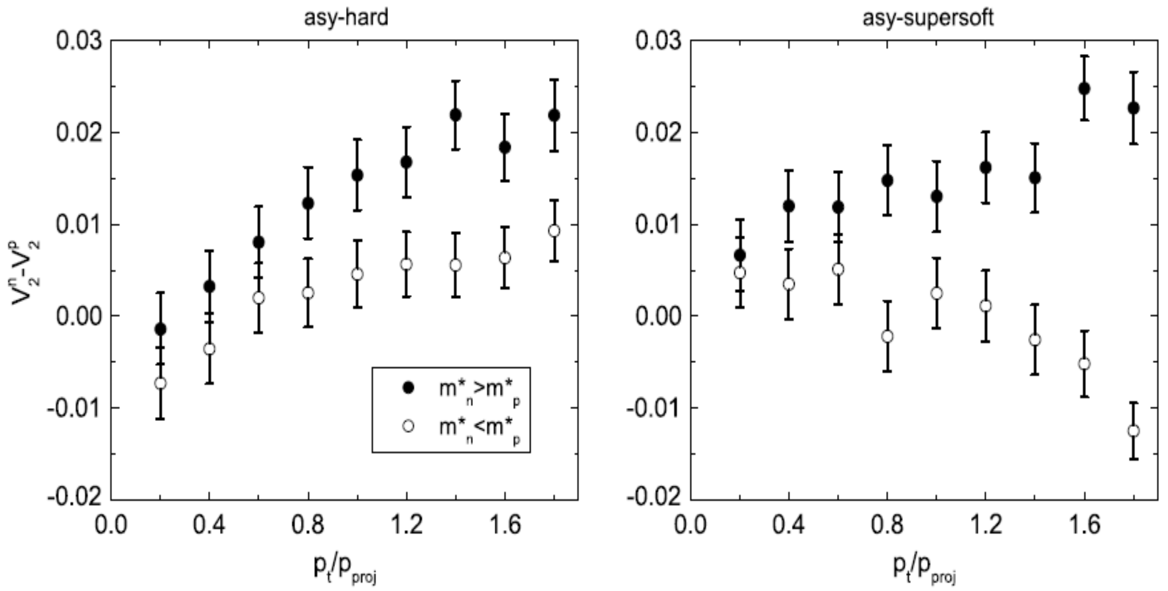

Particle production channels in the LQMD model

π and resonances (Δ(1232), N*(1440), N*(1535), …) production:

$$NN \leftrightarrow N\triangle, \quad NN \leftrightarrow NN^*, \quad NN \leftrightarrow \triangle\triangle, \quad \Delta \leftrightarrow N\pi,$$
$$N^* \leftrightarrow N\pi, \quad NN \leftrightarrow NN\pi(s-state), \quad N^*(1535) \leftrightarrow N\eta$$

Collisions between resonances,

NN*↔NΔ, NN*↔NN*

Strangeness channels:

$$BB \to BYK, \quad BB \to BBK\overline{K}, \quad B\pi \to YK,$$
$$B\pi \to NK\overline{K}, \quad Y\pi \to N\overline{K}, \quad N\overline{K} \to Y\pi, \quad YN \to \overline{K}NN$$

Reaction channels with antiproton:

$$\overline{p}N \to \overline{N}N, \quad \overline{N}N \to \overline{N}N, \overline{N}N \to \overline{B}B, \overline{N}N \to \overline{Y}Y$$
$$\overline{N}N \to \mathtt{annihilation}(\pi, \eta, \rho, \omega, K, \overline{K}, K^*, \overline{K}^*, \phi)$$

Statistical model with SU(3) symmetry for annihilation
(E.S. Golubeva et al., Nucl. Phys. A 537, 393 (1992))

The **PYTHIA** and **FRITIOF** code are used for baryon(meson)-baryon and antibaryon-baryon collisions at high invariant energies

Mean-field potentials for resonances, hyperons and mesons

1. **Mean-field potentials for resonances (Δ(1232), N*(1440), …) are considered based on nucleon potentials, but distinguishing isospin effect.**

$U_{\Delta^{++}} = U_p(\rho, p)$, $U_{\Delta^{+}} = 2U_p(\rho, p)/3 + U_n(\rho, p)/3$, $U_{\Delta^0} = U_p(\rho, p)/3 + 2U_n(\rho, p)/3$, $U_{\Delta^-} = U_n(\rho, p)$

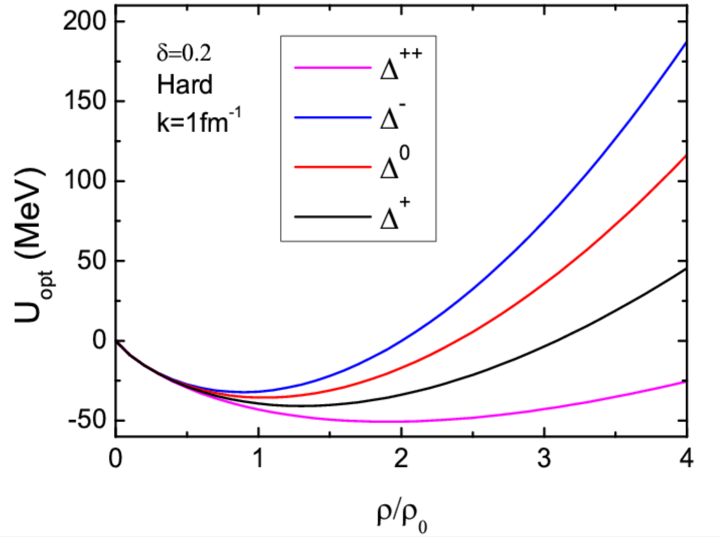

2. Mean-field potentials for hyperons and antiprotons in nuclear medium

$$H_M = \sum_{i=1}^{N_M} \left(V_i^{\mathrm{Coul}} + \omega(\mathbf{p}_i, \rho_i) \right)$$

$$\omega(\mathbf{p}_i, \rho_i) = \sqrt{(m_H + \Sigma_S^H)^2 + \mathbf{p}_i^2} + \Sigma_V^H$$

$$V_{opt}(\mathbf{p}, \rho) = \omega(\mathbf{p}, \rho) - \sqrt{\mathbf{p}^2 + m^2}$$

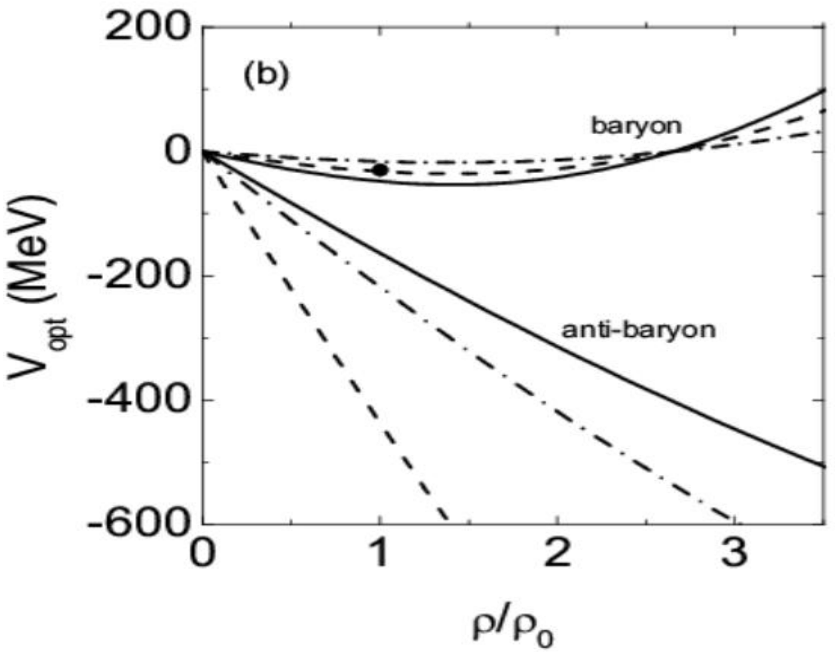

3. Mean-field potentials for pion dynamics

ZQF et al, PRC92, 044604 (2015)

$$\omega_{\tau_z}(\rho, \vec{p}) = \omega_{isoscalar}(\rho, \vec{p}) + C_{iso}^{\pi} \tau_z \delta \left(\frac{\rho}{\rho_0} \right)^{\gamma_\pi}$$

τ_z=1, 0, -1 for π^-, π^0 and π^+

$$\omega_{isoscalar}(\mathbf{p}_i, \rho_i) = S_\pi(\mathbf{p}_i, \rho_i)\omega_{\pi\text{-}like}(\mathbf{p}_i, \rho_i) + S_\Delta(\mathbf{p}_i, \rho_i)\omega_{\Delta\text{-}like}(\mathbf{p}_i, \rho_i)$$

$$S_\pi(\mathbf{p}_i, \rho_i) + S_\Delta(\mathbf{p}_i, \rho_i) = 1$$

$$S(\mathbf{p}_i, \rho_i) = \frac{1}{1 - \partial\Pi(\omega)/\partial\omega^2}$$

Details in PRC47 (1993) 788, 55 (1997) 411

The energy balance in the decay of resonance

$$\sqrt{m_R^2 + \mathbf{p}_R^2} = \sqrt{m_N^2 + (\mathbf{p}_R - \mathbf{p}_\pi)^2} + \omega_\pi(\mathbf{p}_\pi, \rho)$$

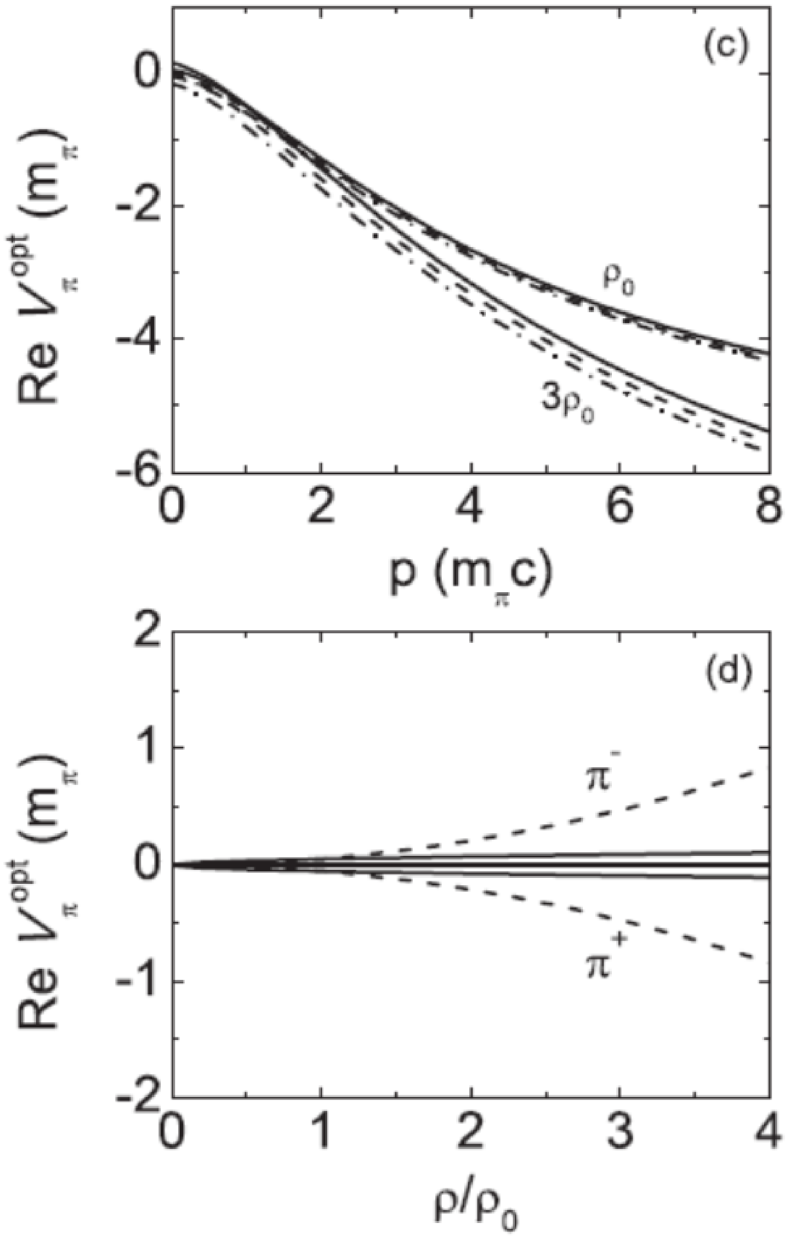

4. Mean-field potentials for η transport (J. Chen, Z. Q. Feng et al., Eur. Phys. J. A (2017) 53: 128)

$$\omega_\eta = \sqrt{\left(m_\eta^2 - \frac{\Sigma_{\eta N}}{f^2}\rho_s\right)\left(1+\frac{\kappa}{f^2}\rho_s\right)^{-1} + p^2}$$

$$V_\eta^{opt} = \omega_\eta^*(\mathbf{p}_i,\rho_i) - \omega_\eta(\mathbf{p}_i,\rho_i) = \sqrt{(m_\eta^*)^2+\mathbf{p}_i^2} - \sqrt{m_\eta^2+\mathbf{p}_i^2}$$

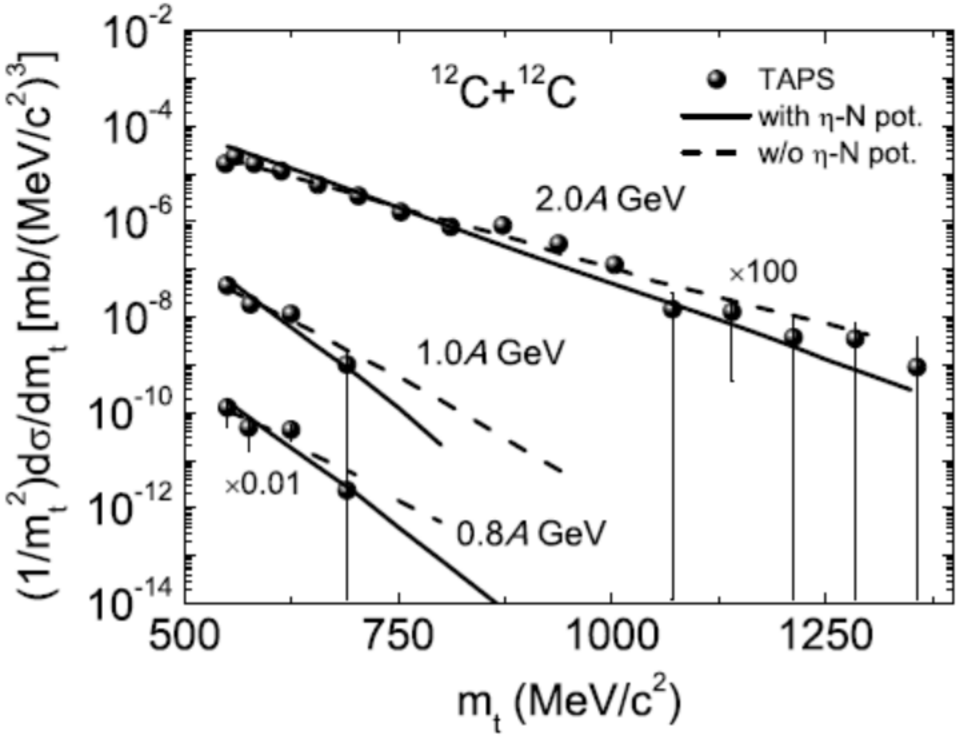

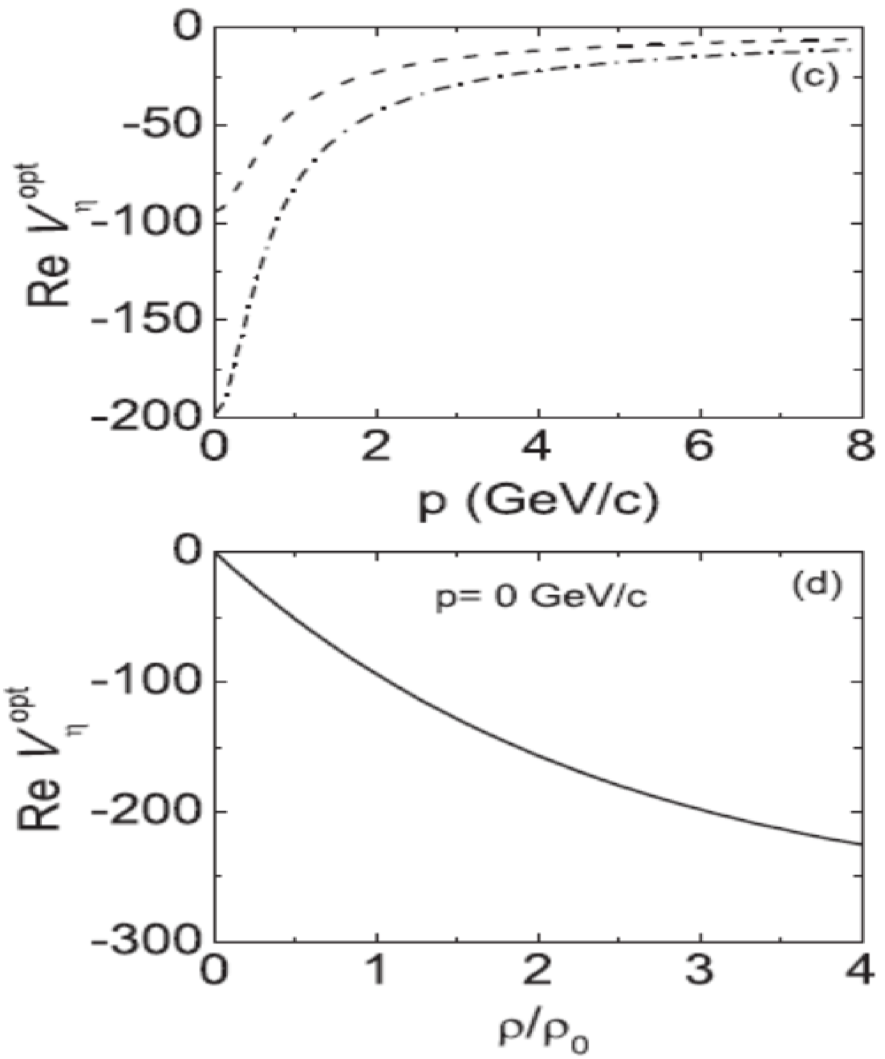

5. Mean-field potentials for kaons and antikaons

J.Schaffner-Bielich et al., Nucl. Phys. A 625 (1997) 325, Z. Q. Feng, Nucl. Phys. A 919 (2013) 32-45

$$\omega_K(\mathbf{p}_i,\rho_i) = \left[m_K^2 + \mathbf{p}_i^2 - a_K\rho_i^S - \tau_3 c_K \rho_{i3}^S + (b_K\rho_i + \tau_3 d_K \rho_{i3})^2\right]^{1/2} + b_K\rho_i + \tau_3 d_K \rho_{i3}$$

$$\omega_{\overline{K}}(\mathbf{p}_i,\rho_i) = \left[m_{\overline{K}}^2 + \mathbf{p}_i^2 - a_{\overline{K}}\rho_i^S - \tau_3 c_K \rho_{i3}^S + (b_K\rho_i + \tau_3 d_K \rho_{i3})^2\right]^{1/2} - b_K\rho_i - \tau_3 d_K \rho_{i3}$$

$b_K = 3/(8f_\pi^{*2}) \approx 0.333$ GeV fm^3 with assuming $f_\pi^* = f_\pi$, the a_K and $a_{\overline{K}}$ are 0.18 GeV^2 fm^3 and 0.31 GeV^2 fm^3, respectively,
The parameters $c_K = 0.0298$ GeV^2 fm^3 and $d_K = 0.111$ GeV fm^3

$$\frac{d\mathbf{p}_i}{dt} = -\frac{\partial V_i^{\mathrm{Coul}}}{\partial \mathbf{r}_i} - \frac{\partial \omega_{K(\overline{K})}(\mathbf{p}_i,\rho_i)}{\partial \mathbf{r}_i} \pm \mathbf{v}_i \frac{\partial \mathbf{V}_i}{\partial \mathbf{r}_i}$$

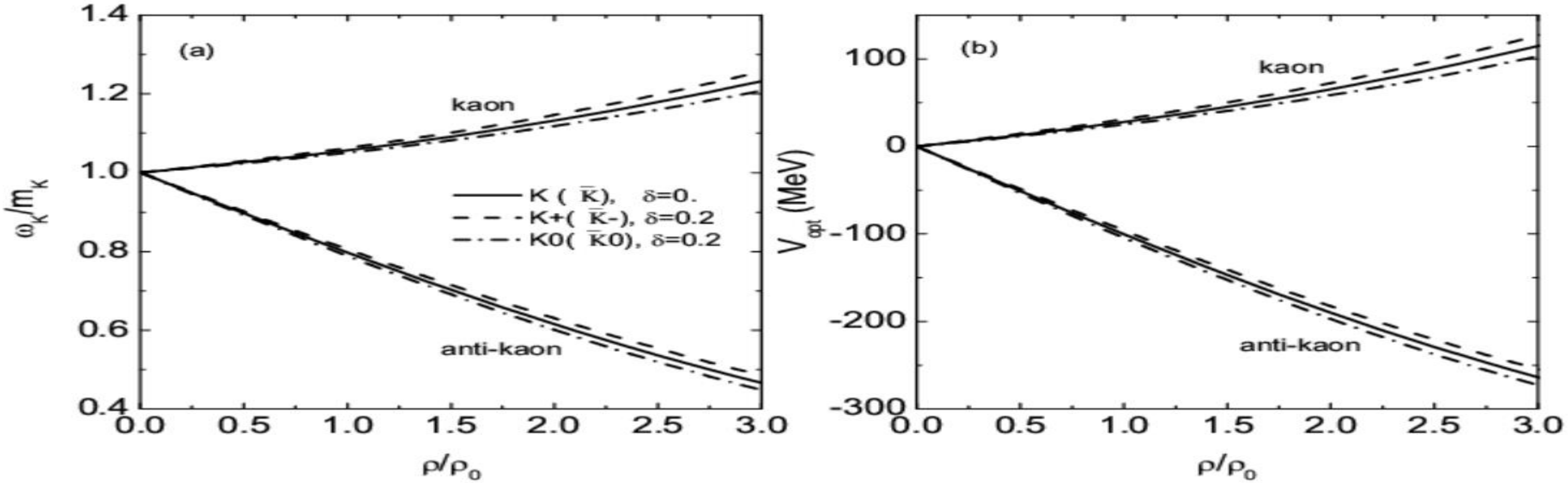

$V_{K+}(\rho_0)$= 28 MeV, $V_{K-}(\rho_0)$= -100 MeV

III. (1) Particle production in HICs

Particle production π, K, Λ and Σ in the reaction ^{197}Au+^{197}Au at 1.5A GeV **(Phys. Rev. C 82 (2010) 057901)**

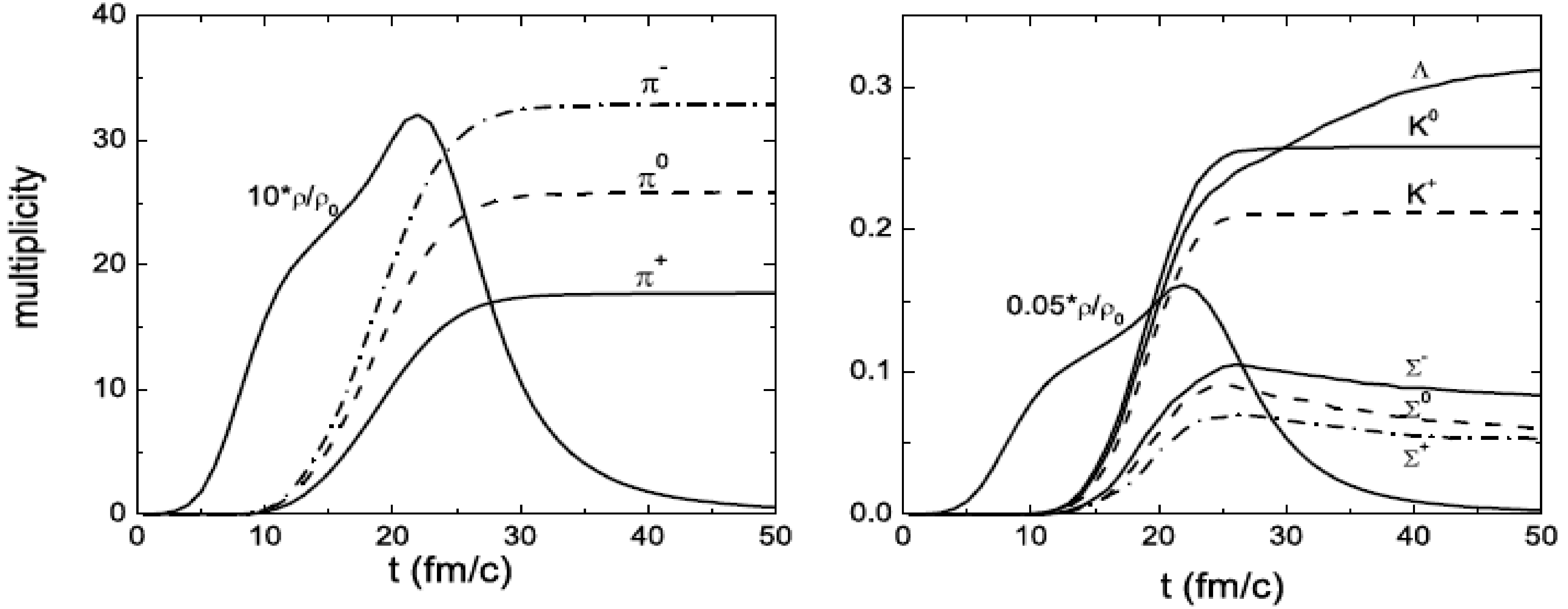

In-medium modifications on elementary cross section via effective mass, e.g., πN→KY

$$\sqrt{s_{th}} = m_Y^* + m_K^*$$

Threshold energies for $E_{th}(\pi^0)$= 0.28 GeV, $E_{th}(\eta)$= 1.25 GeV, $E_{th}(K^+)$= 1.58 GeV, $E_{th}(K^-)$= 2.5 GeV

Temporal evolution of production rate and density profiles of particles in collisions of $^{197}Au+^{197}Au$

Nucl. Sci. Tech. 29, 40 (2018)

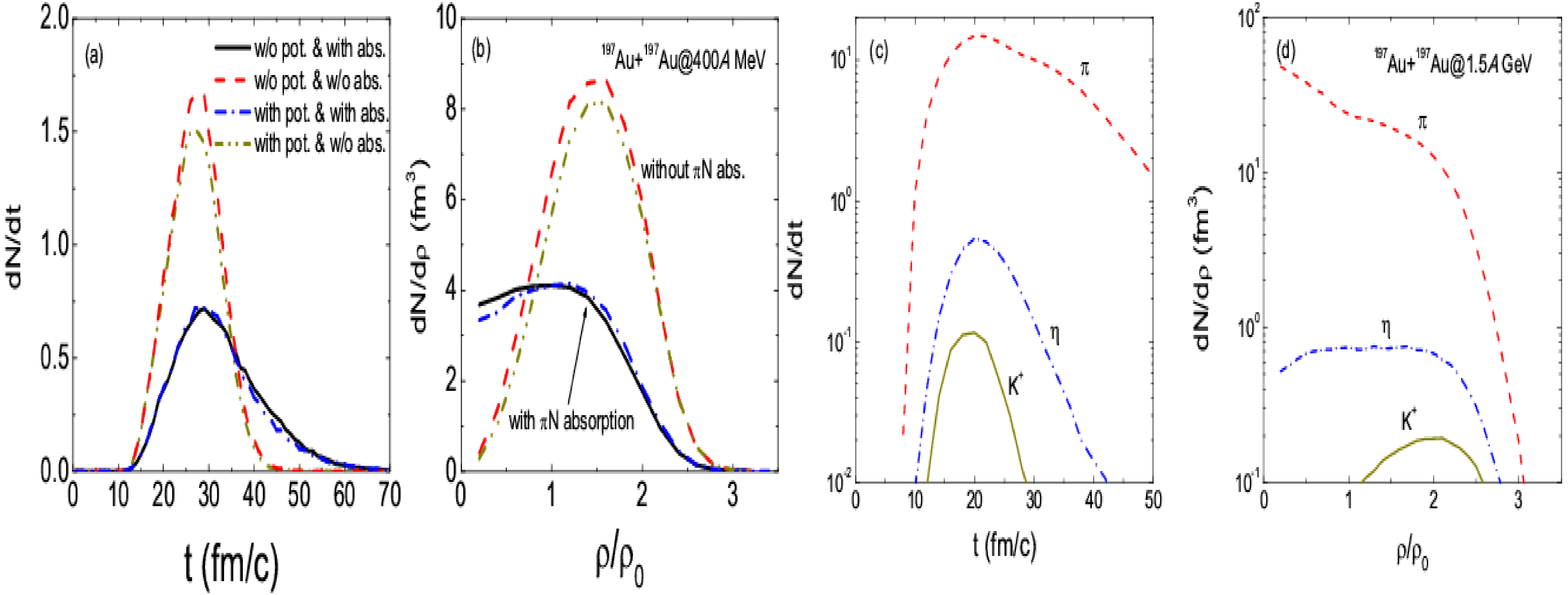

Production of neutral particles in central ^{40}Ca+ ^{40}Ca collisions

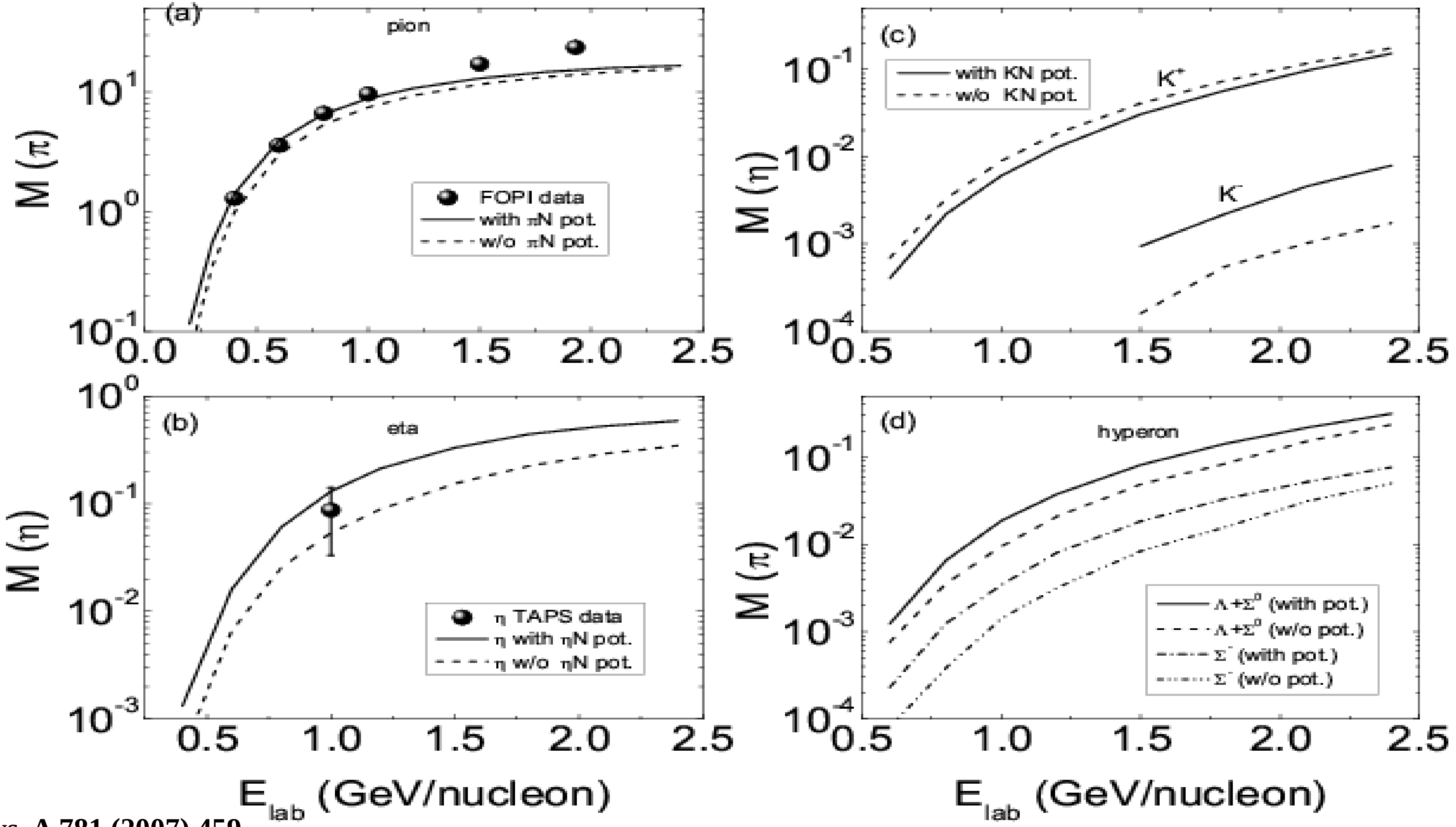

FOPI: Nucl. Phys. A 781 (2007) 459
TAPS: Phys. Rev. C 67 (2003) 024903

The ratio of K^-/K^+ as a function of transverse mass (kinetic energy) in collisions of ^{12}C + ^{12}C and protons on ^{12}C and ^{197}Au at the beam energies of 1.8*A* GeV and 2.5 GeV, respectively.

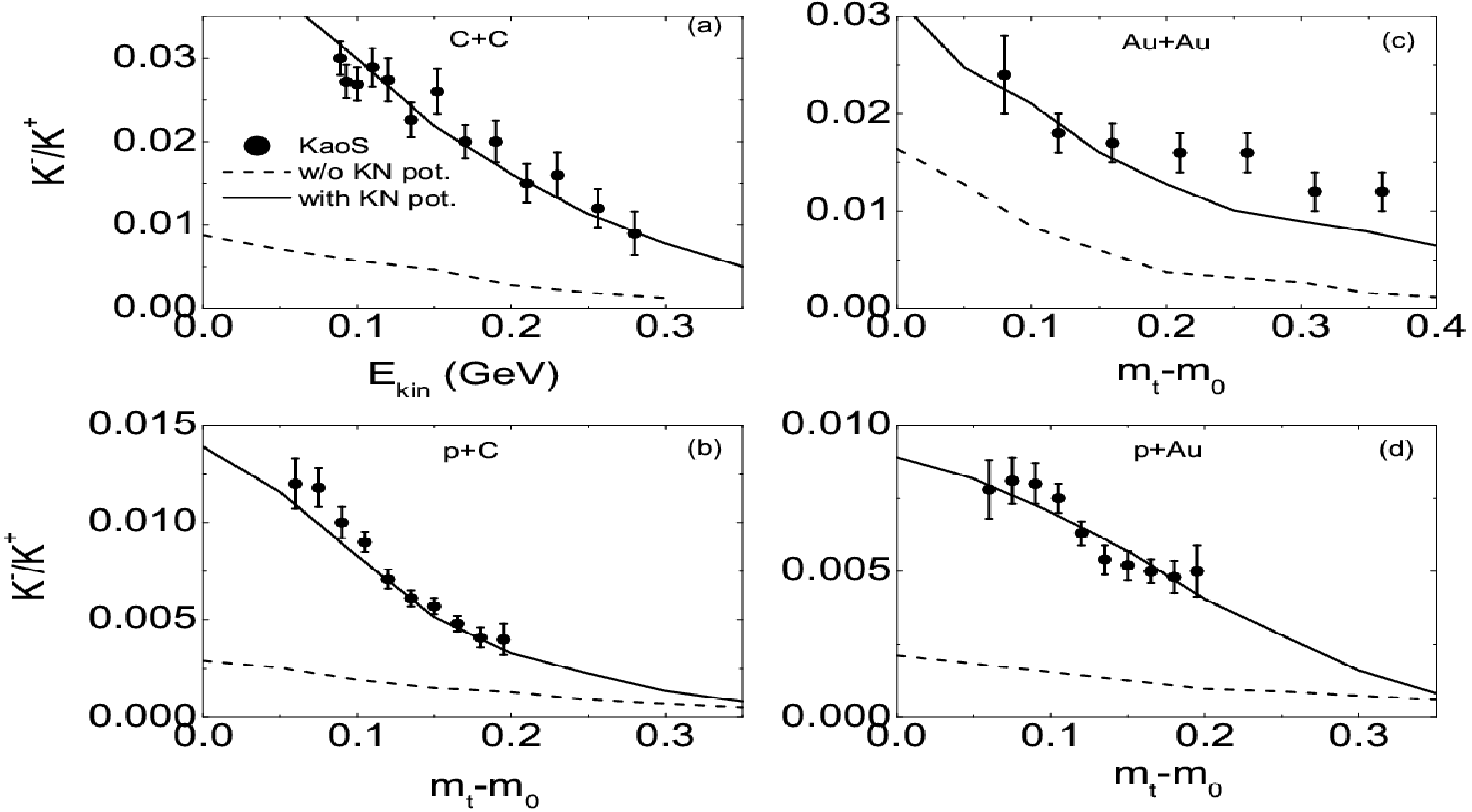

$V_{K+}(\rho_0)$= 28 MeV, $V_{K-}(\rho_0)$= -100 MeV

Antiproton production in HICs

$E_{th}(\bar{p})$= 5.62 GeV

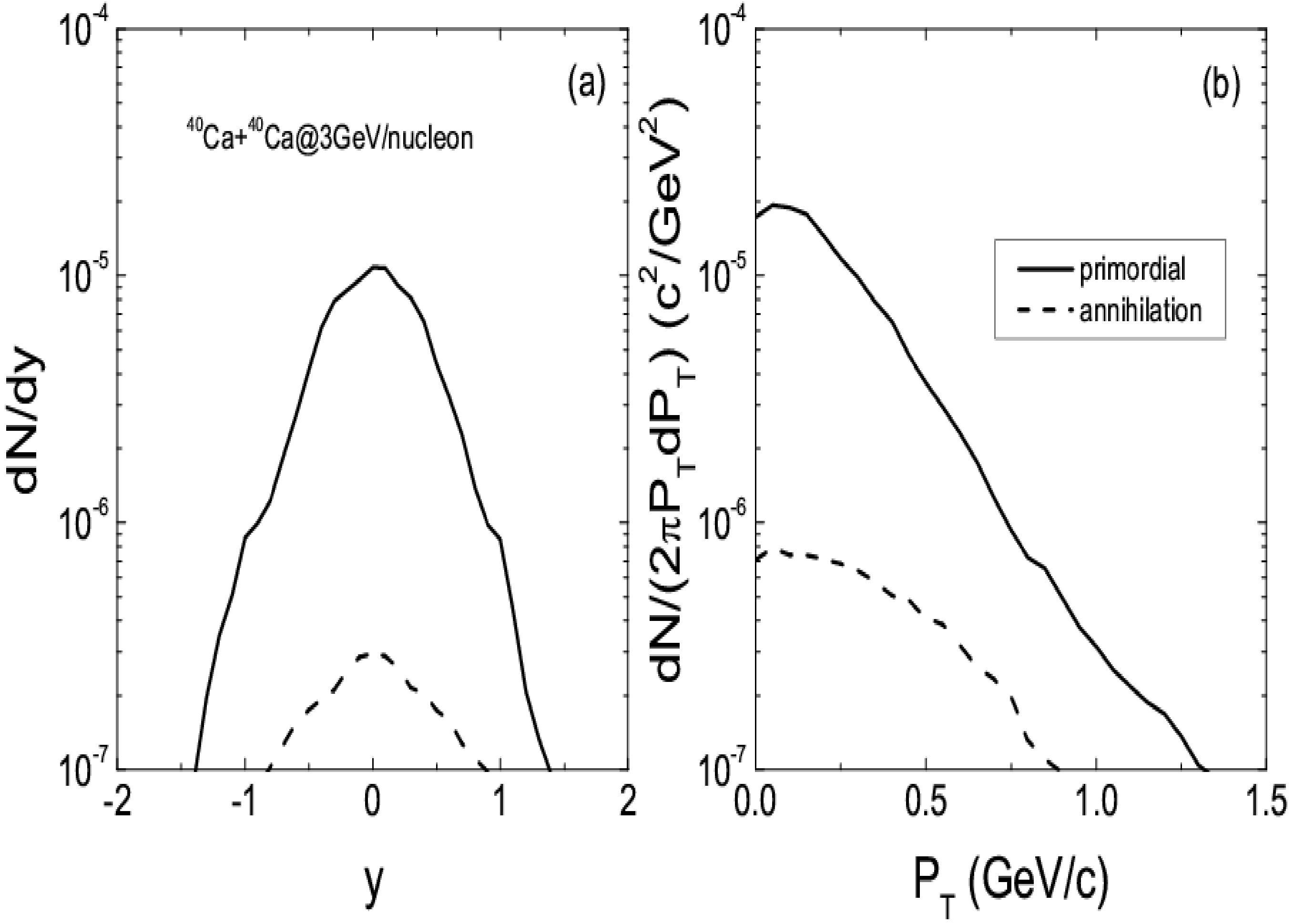

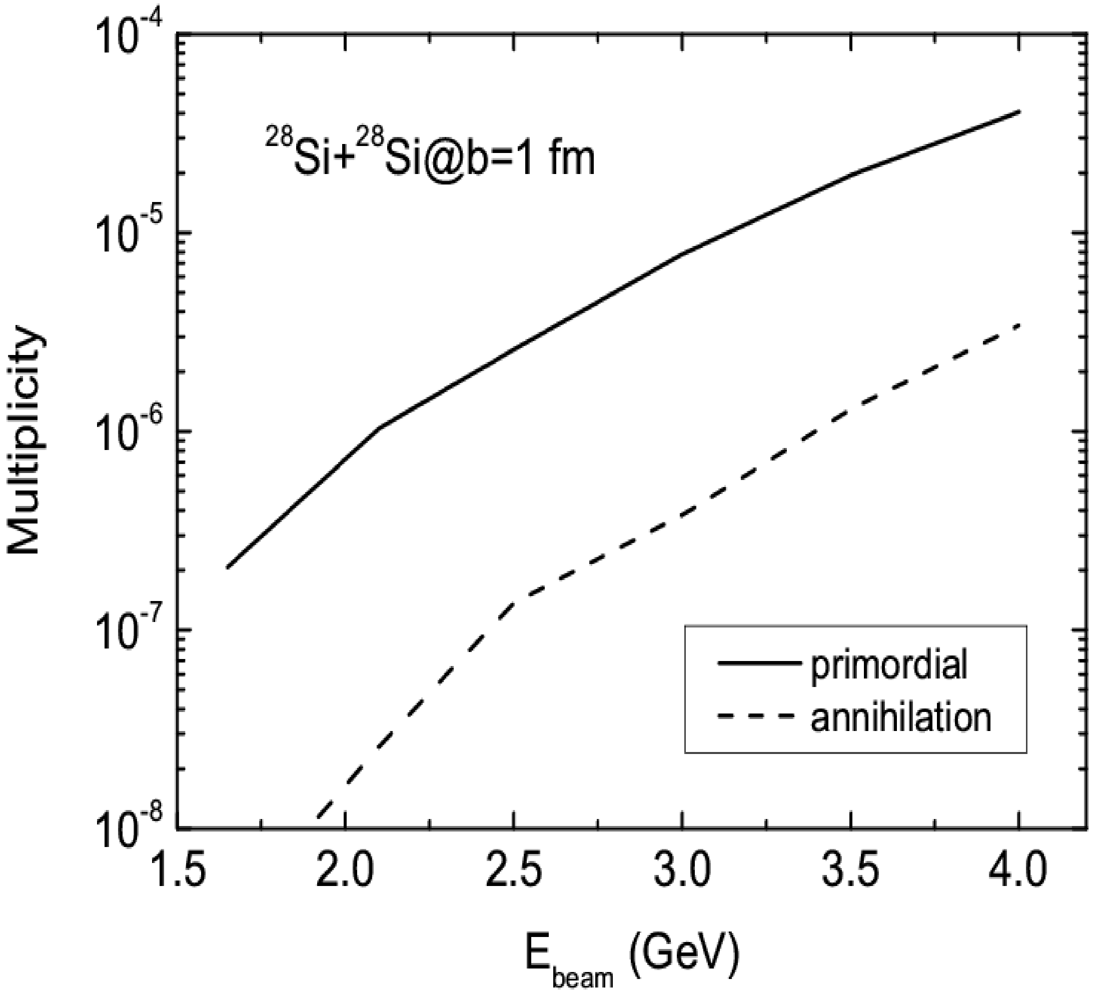

III. (2) K⁻ induced nuclear ractions

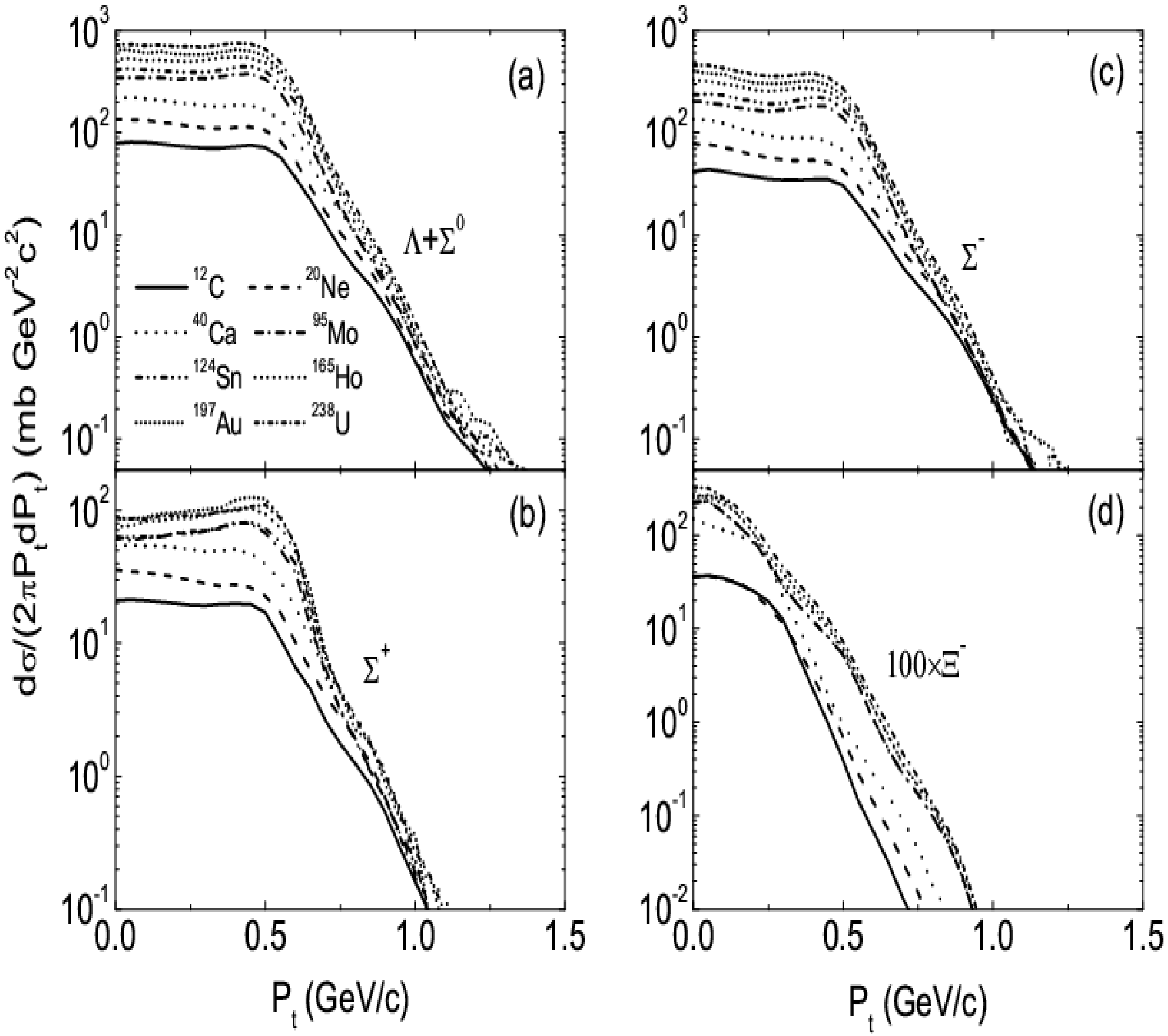

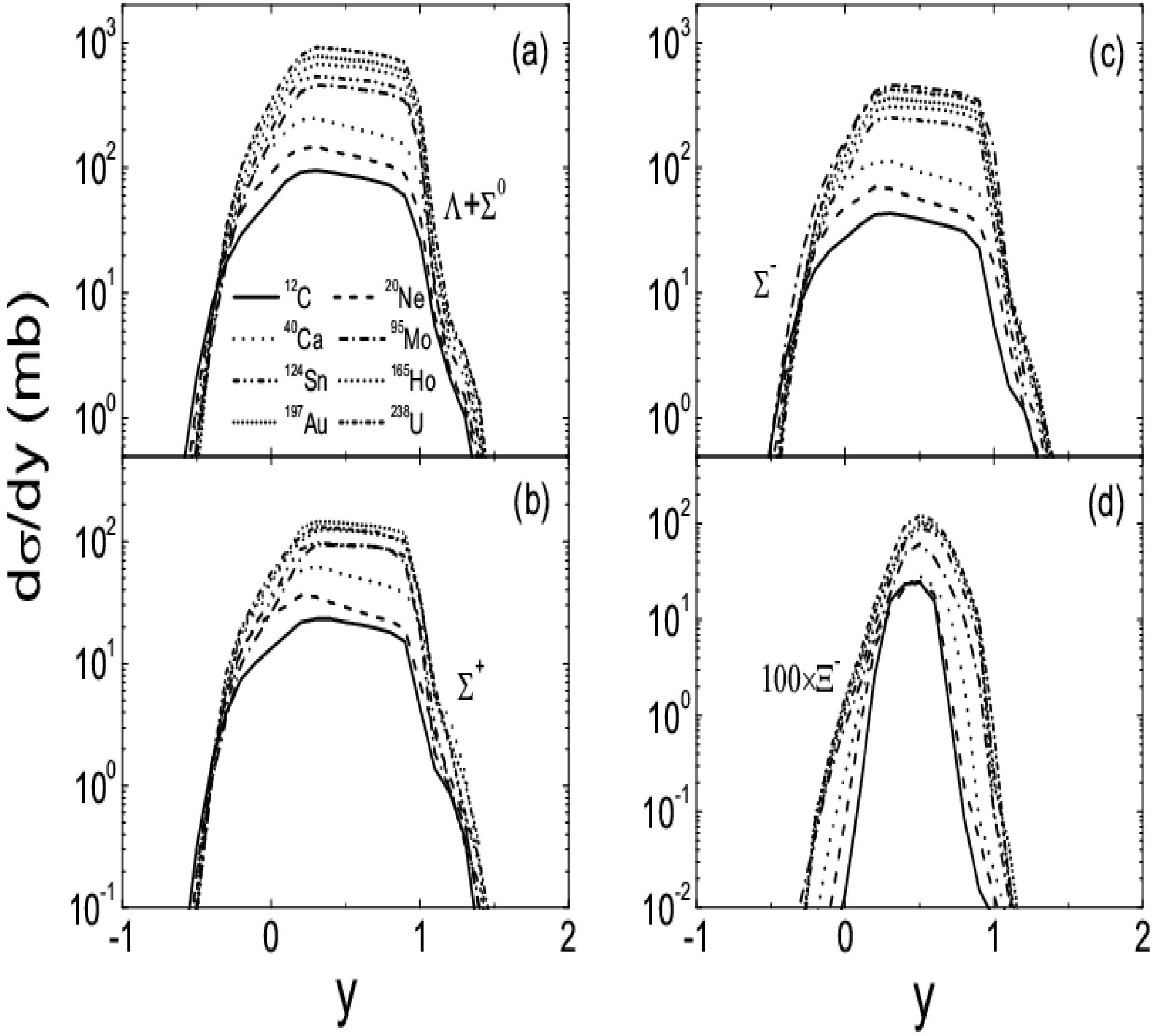

III. (3) antiproton induced reactions

Z. Q. Feng and H. Lenske, Phys. Rev. C 89, 044617 (2014)

$\bar{p}+^{40}Ca$, 4 GeV/c

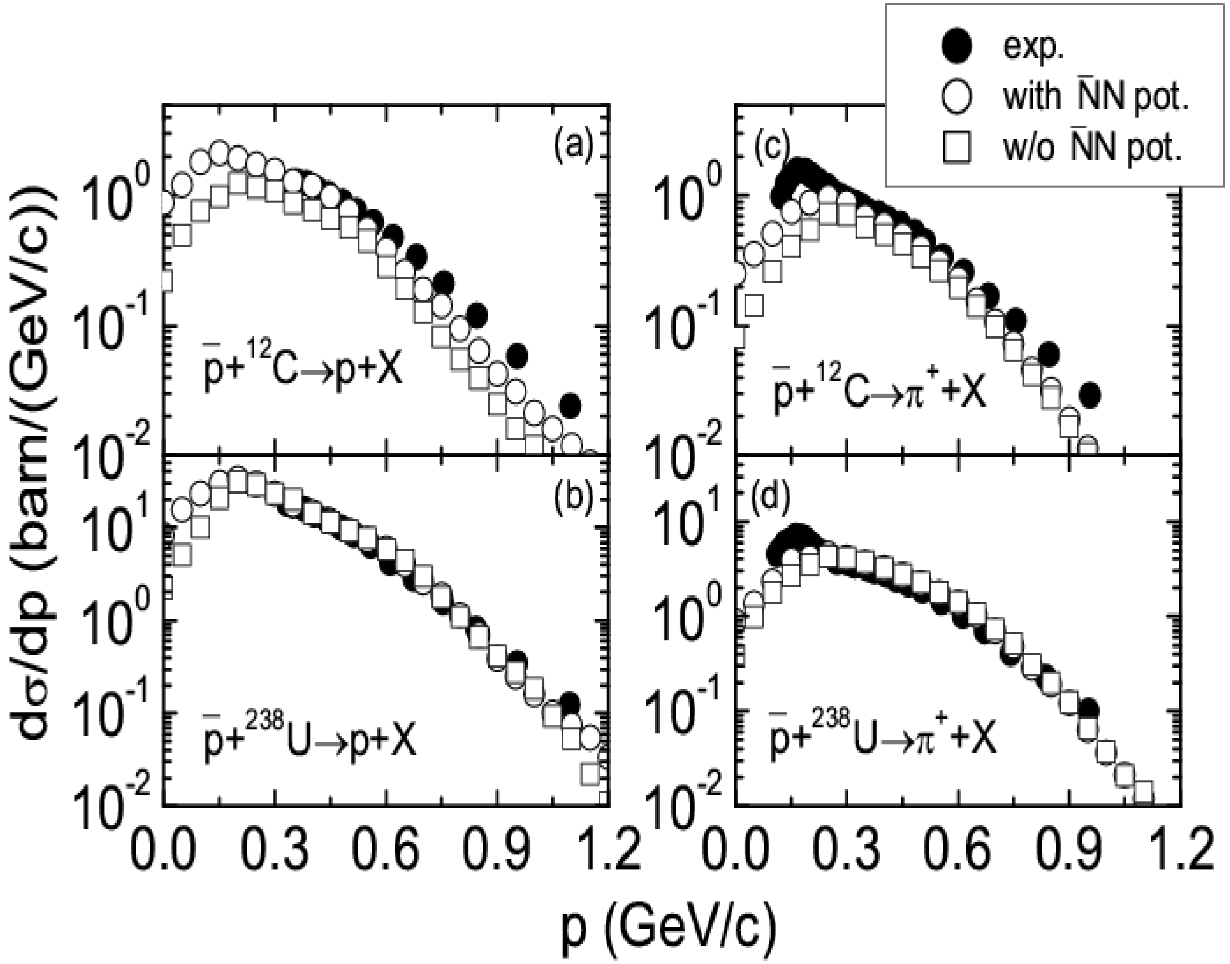

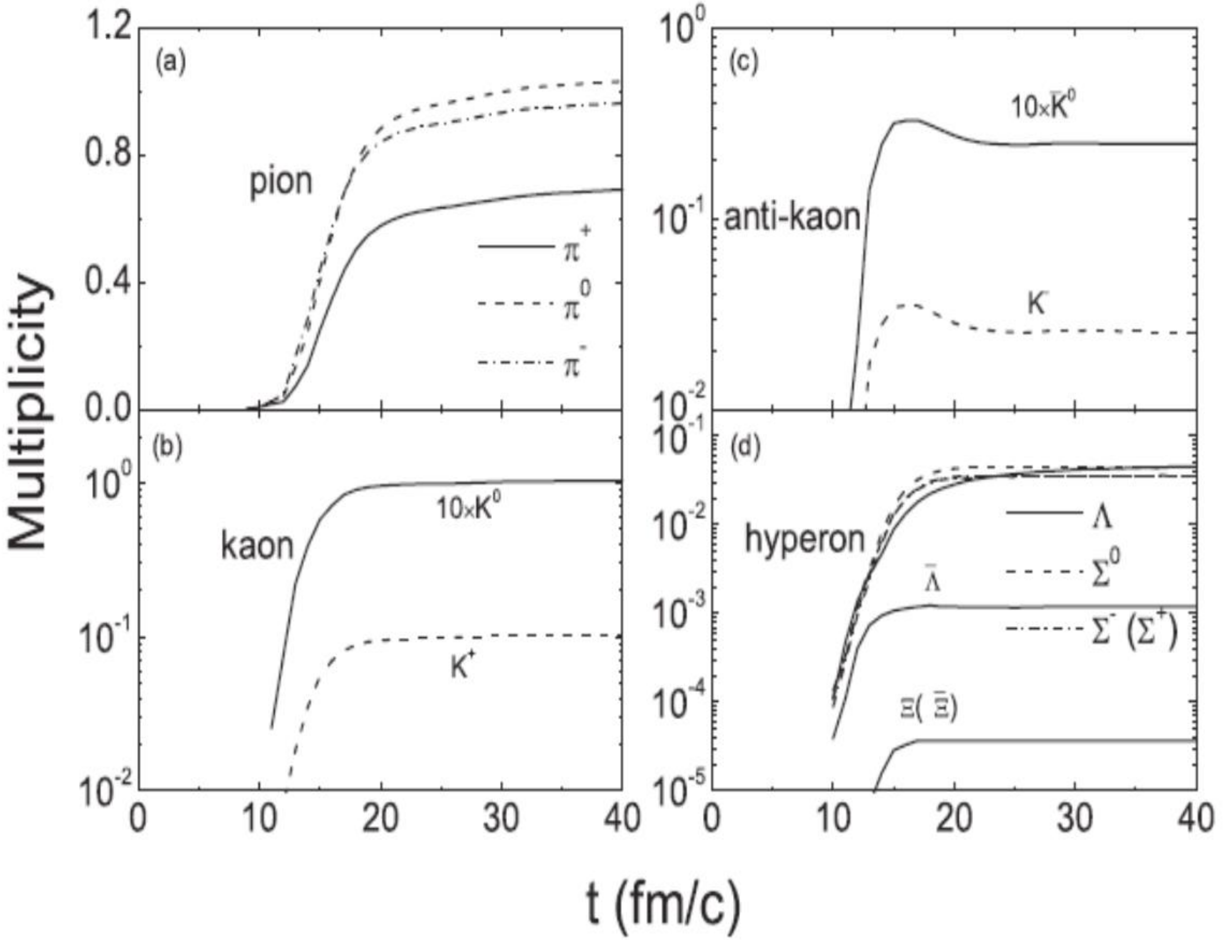

LEAR (Low-Energy Antiproton Ring) at CERN (P. L. McGaughey et al., Phys. Rev. Lett. 56, 2156 (1986))

III. (4) Isospin effects in HICs

Zhao-Qing Feng, Phys. Rev. C 94, 014609 (2016)

The yields of free nucleons and 'gas-phase' nucleons (nucleons, hydrogen and helium isotopes) from the neck fragmentations at the fermi energy of 35 MeV/nucleon within the collision centralities of 6-8 fm

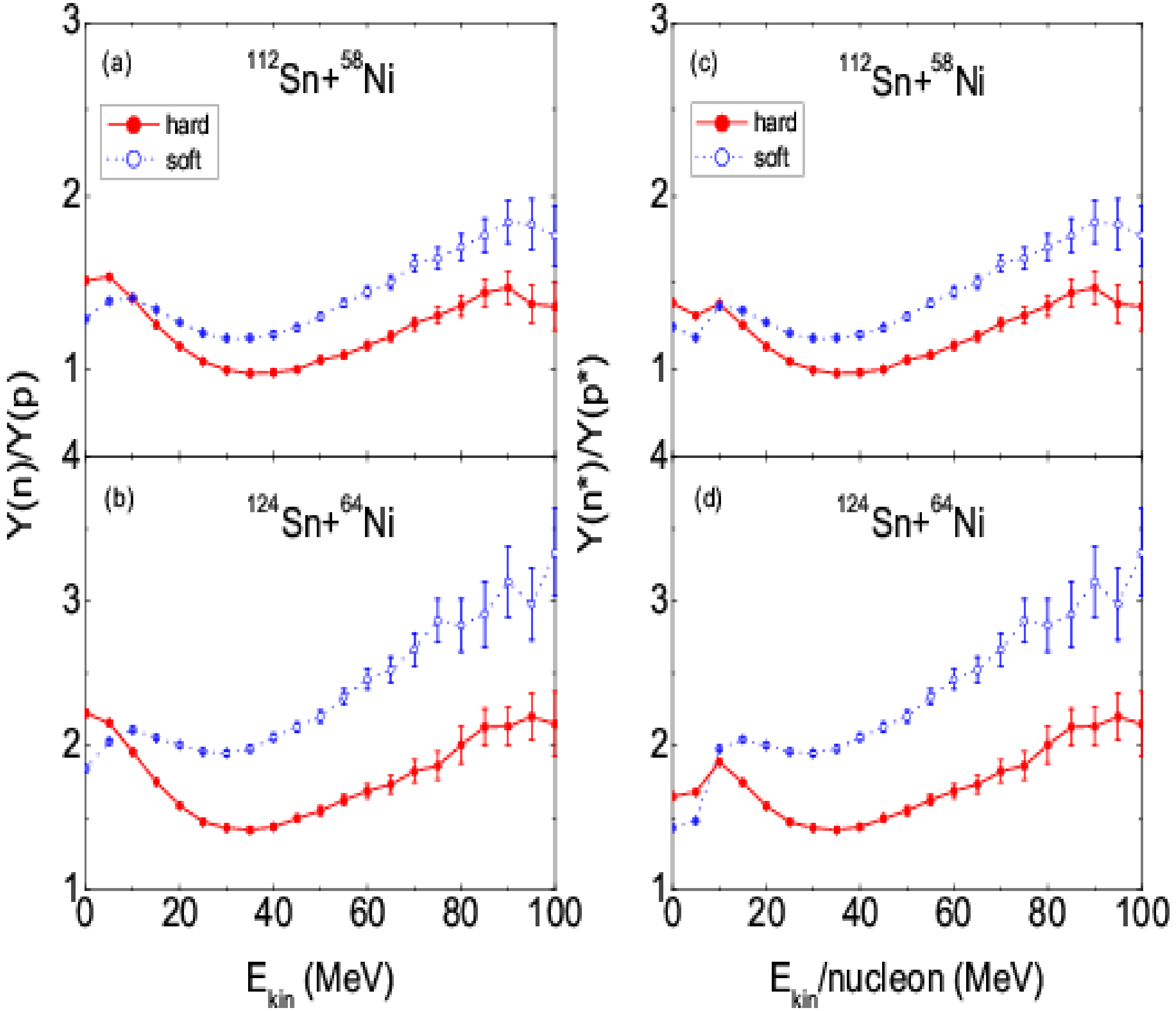

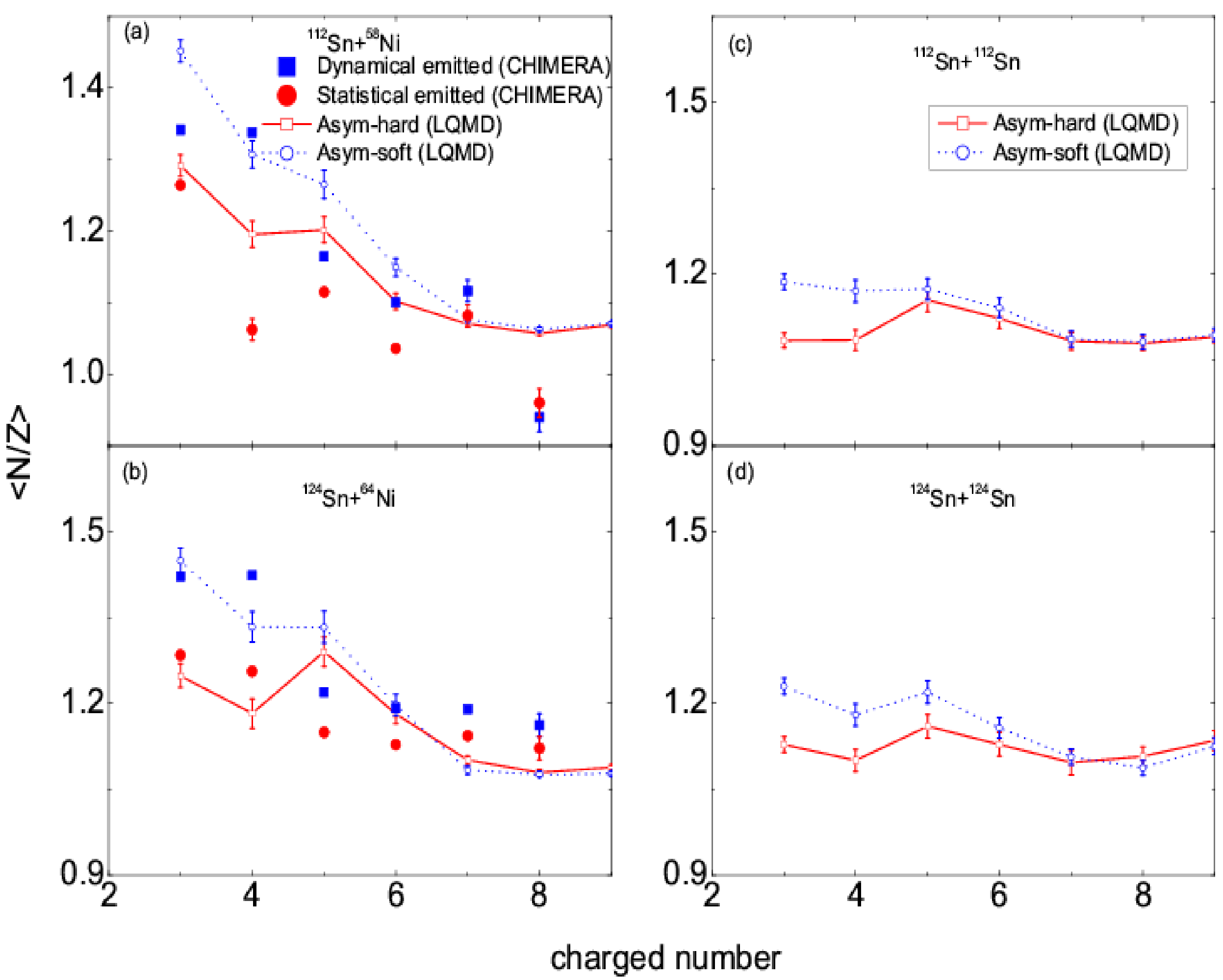

III. (5) Hypernuclear formation in HICs

科学通报 2018 年 第 63 卷 第 8 期: 735～744
论 文
《中国科学》杂志社 SCIENCE CHINA PRESS

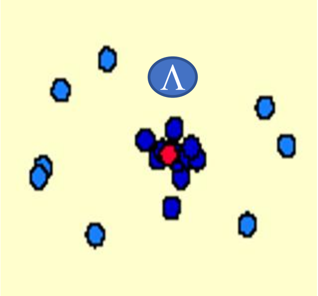

中高能重离子碰撞中奇异粒子产生和超核形成机制

冯兆庆
中国科学院近代物理研究所, 兰州 730000
E-mail: fengzhq@impcas.ac.cn

Classical coalescence approach

The rapidity and kinetic energy distributions of nucleonic fragments, Λ-hypernuclide fragments and free hyperons

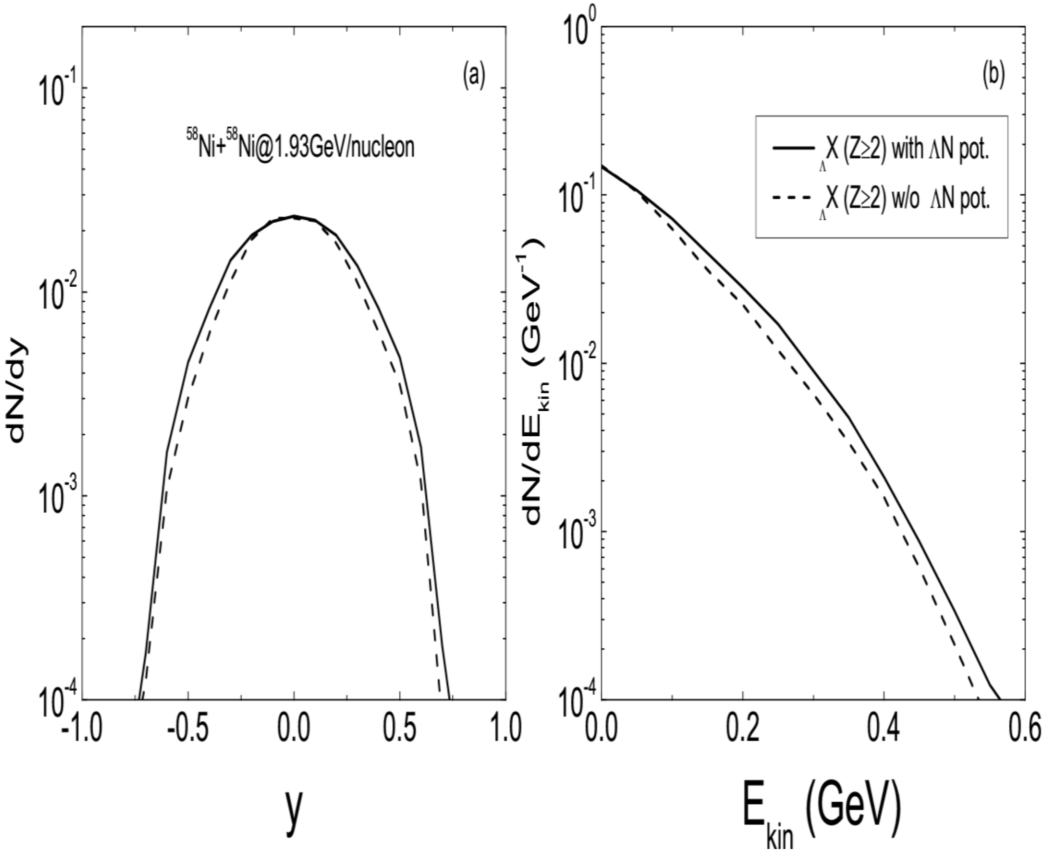

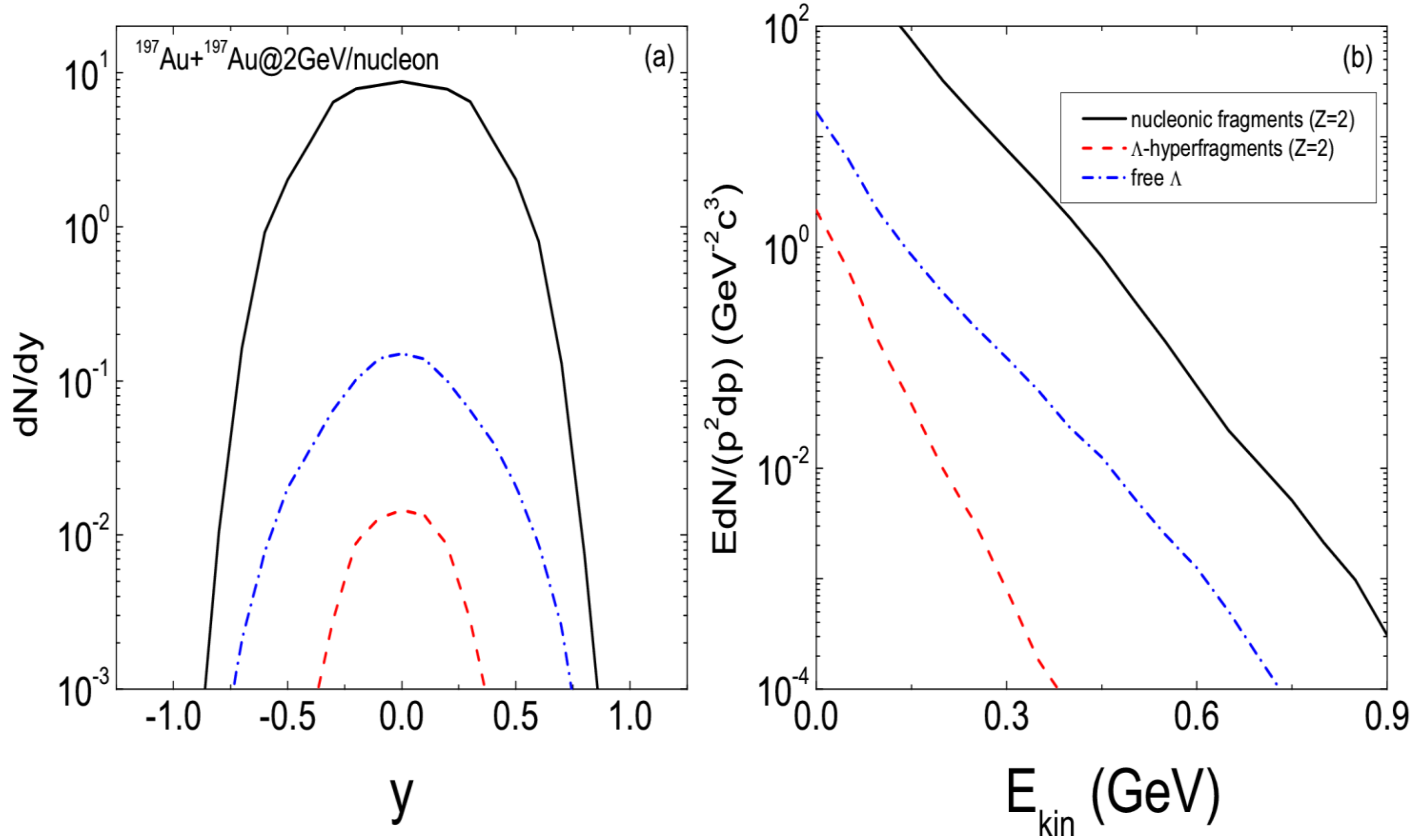

Production of Λ-hypernuclide in $^{197}Au+^{197}Au$ at the beam energy of 2 GeV/nucleon

Nuclear Science and Techniques 29 (2018) 40

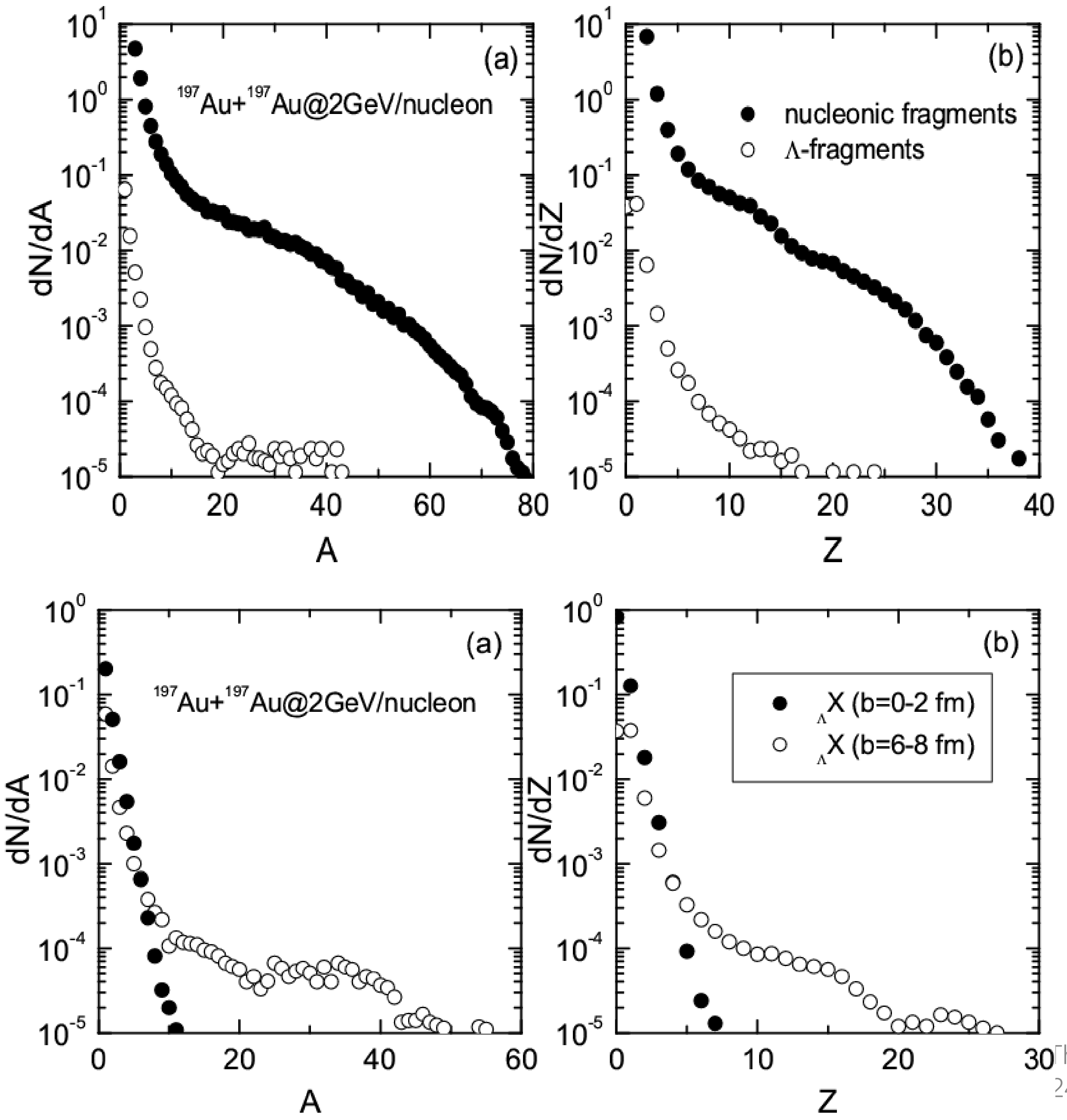

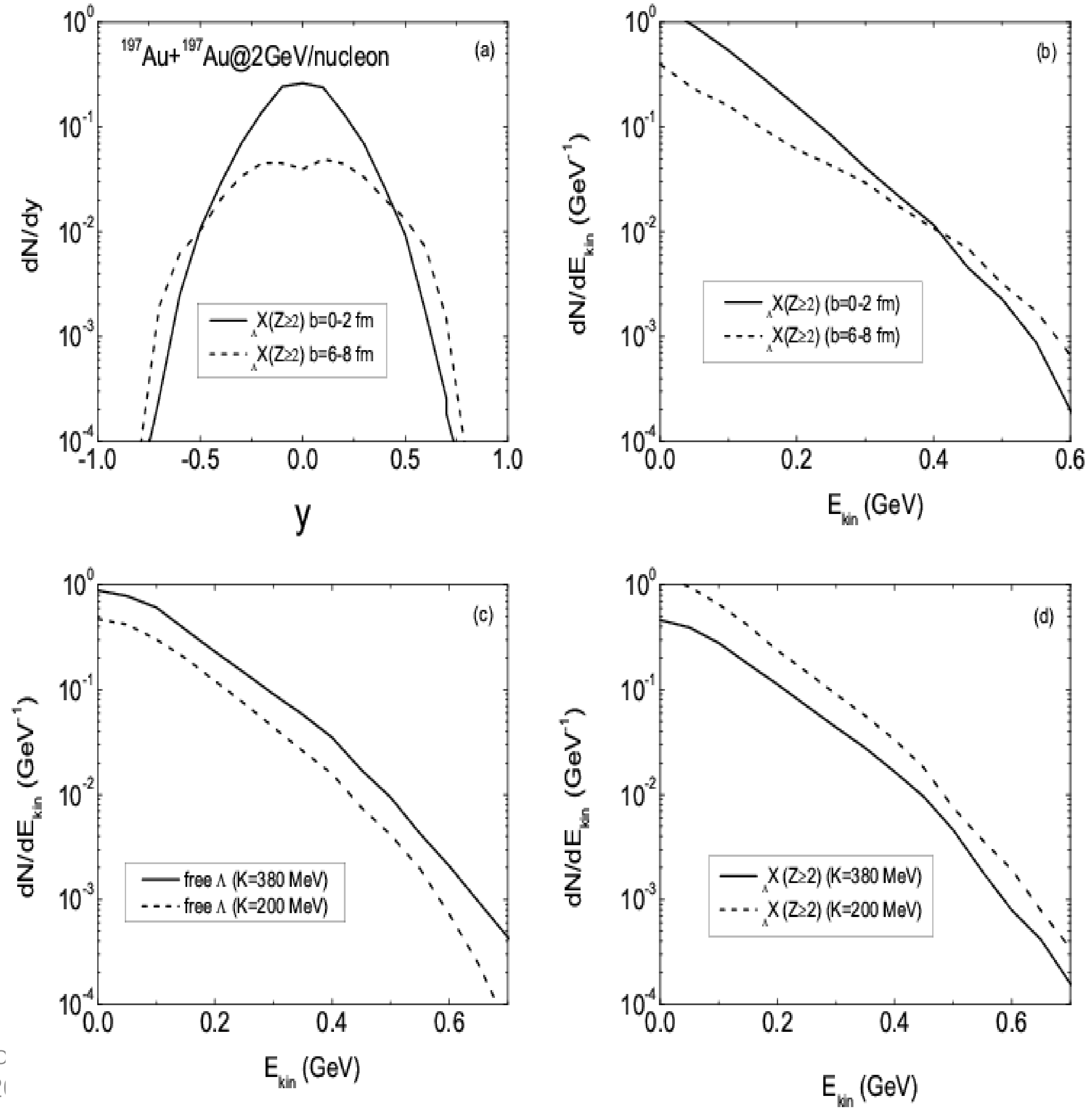

III. (6) Hypernuclear formation in antiproton induced reactions

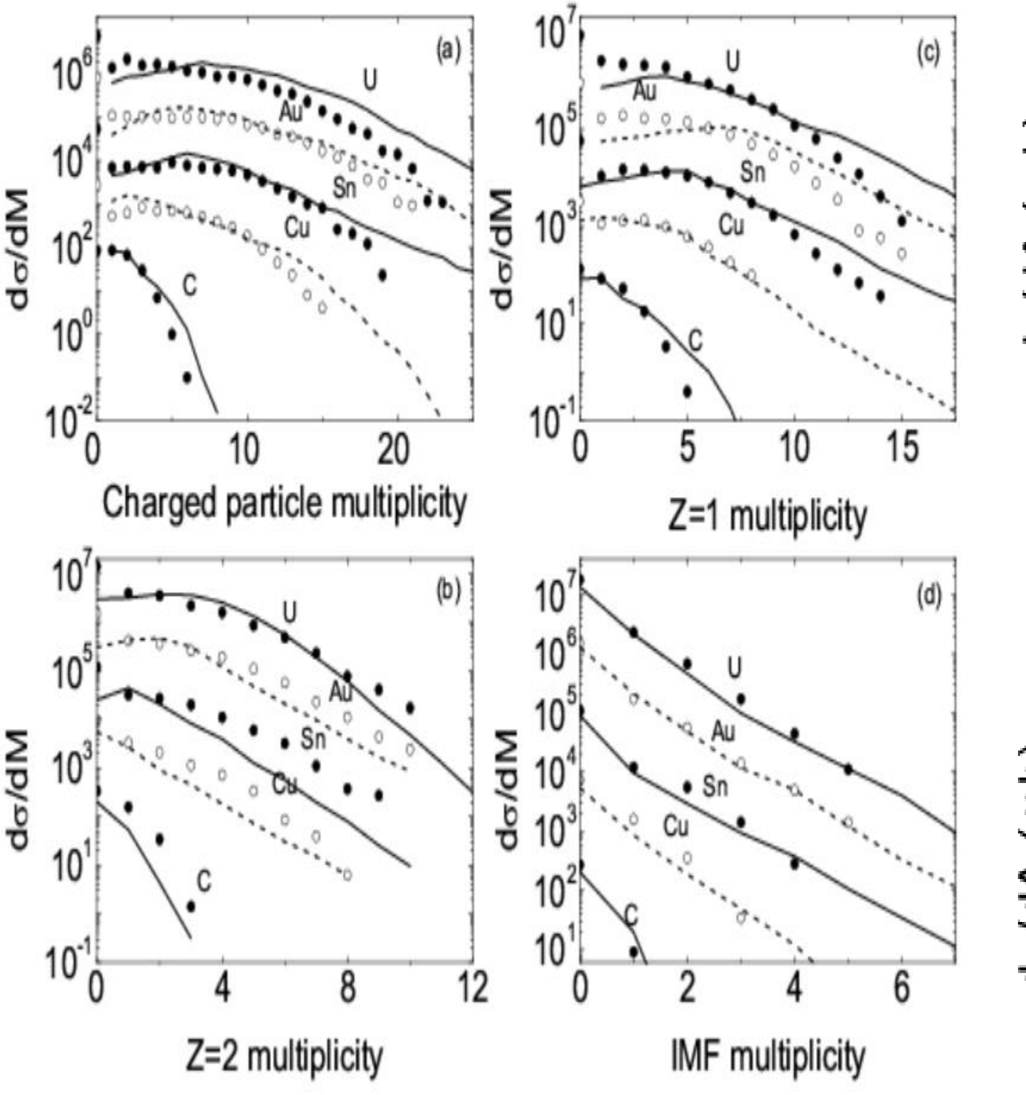

Phys. Rev. C 93, 041601(R) (2016)

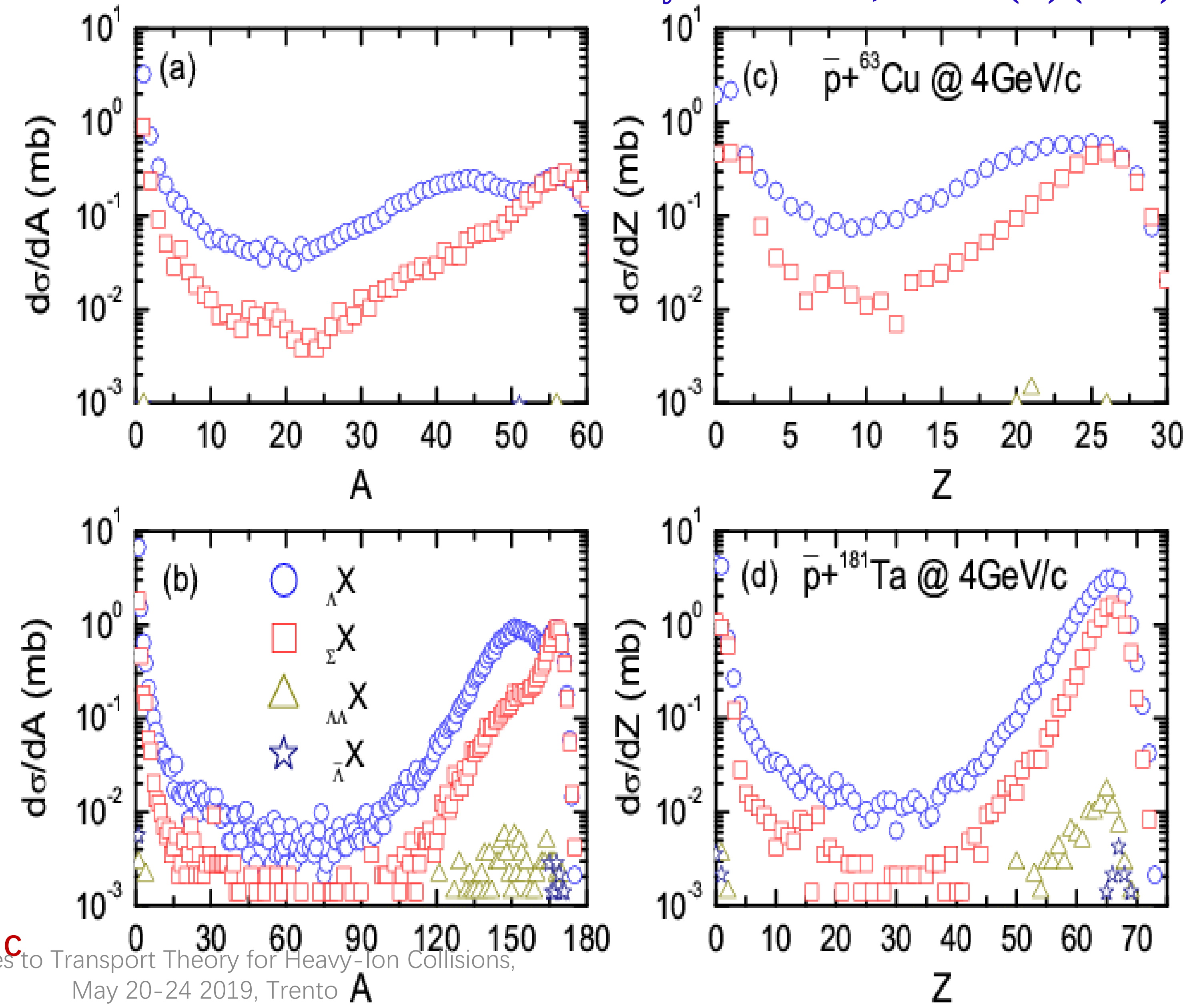

Experimental data: LEAR at CERN, B. Lott *et al.*, Phys. Rev. C 63, 034616 (2001) with 1.22 GeV antiproton

III. (7) Hypernuclear formation in K$^-$ induced reactions

K$^-$+^{40}Ca

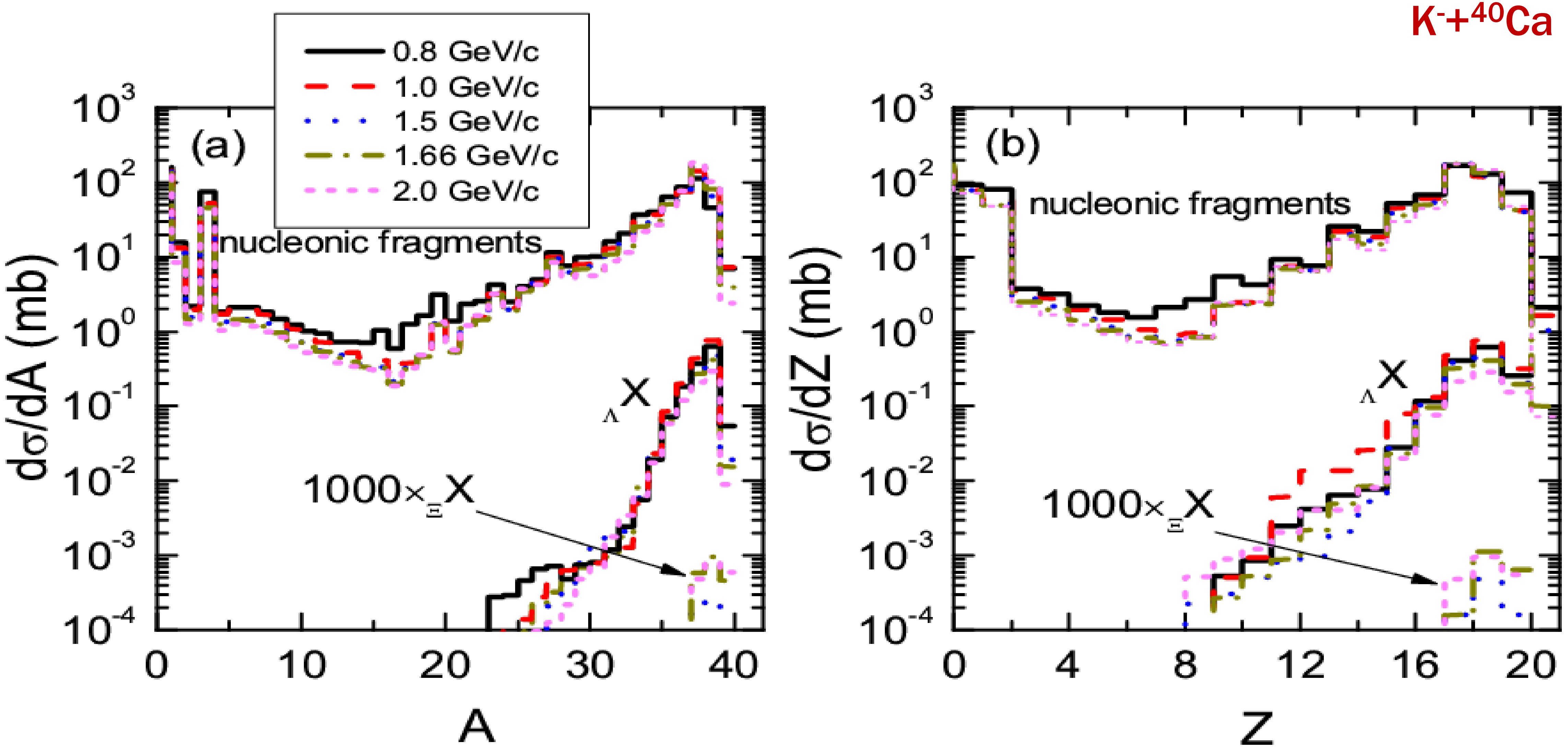

VI. Summary

- Dynamics of strange particles and hypernuclear formation in heavy-ion collisions near threshold energies have been investigated by using the LQMD transport model.
- The mean-field potentials and in-medium modifications on elementary cross sections are of importance on particle emission in phase space. The available experimental data can ben well understood within inclusion of the mean-field potentials.
- Dynamics of hypernuclide formed in heavy-ion collisions and in antiproton (K-) induced reactions is discussed and proposed in the future experiments.

Thank you for your attention!